Weierstraß-Institut
für Angewandte Analysis und Stochastik

im Forschungsverbund Berlin e.V.

Preprint ISSN 0946 – 8633

Sharp-interface model for eutectic alloys
Part I: Concentration dependent surface tension

W. Dreyer, B. Wagner [1]

submitted: 13. Nov. 2003

[1] Weierstrass Institute for Applied Analysis and Stochastics
Mohrenstrasse 39
D – 10117 Berlin
Germany
E-Mail: wagnerb@wias-berlin.de, dreyer@wias-berlin.de

No. 885
Berlin 2003

1991 *Mathematics Subject Classification.* 74D10,74F05,74F10,77N25.

Key words and phrases. Matched asymptotics, boundary integral method, numerics.

Edited by
Weierstraß-Institut für Angewandte Analysis und Stochastik (WIAS)
Mohrenstraße 39
10117 Berlin
Germany

Fax: + 49 30 2044975
E-Mail: preprint@wias-berlin.de
World Wide Web: http://www.wias-berlin.de/

Abstract

We consider the problem of phase separation in eutectic alloy such e.g. $SnPb$. For this we derive a phase field model from an atomistic point of view. We find the surface energy to be anisotropic, having in general a nonlinear dependence on concentration. We use matched asymptotic analysis to obtain a corresponding sharp interface model. The resulting expression for the surface tension agrees with that found on the basis of classical thermodynamics for jump conditions at singular interfaces. A boundary integral formulation of the sharp interface model enables us to numerically describe the motion and deformation of the binary alloy.

1 Introduction

Already in 1958 J. W. Cahn and J. E. Hilliard [1] considered the possibility of anisotropic surface tension in a crystal lattice. This is generically the case when modelling phase separation in multi-phase systems such as binary alloys. A number of models have been developed generalizing the Cahn-Hilliard equation to multi-component systems by introducing a vector valued order parameter and by making some general assumptions on the form of the gradient energy, [4], [20], [19]. Using matched asymptotic expansions, corresponding sharp-interface models were then developed and expressions for surface tension were determined on the basis of results by Herring on anisotropic surface energy, [11], [15].

Recently, a phase field model for the description and simulation of coarsening processes occuring in binary alloys, that are caused by diffusion in local inhomogeneous stress fields, has been formulated by W. Dreyer and W.H. Müller, [5]. There, the model is applied to the eutectic solder alloy consisting of lead and tin. Figure 1 shows a typical morphology that developed from an initially fine mix of alternating layers of lead-rich and tin-rich regions after 20 hours of slow cooling. The regions are resolved on a μm -scale. This coarsening process is initiated by diffusion subjected to the effects of anisotropic surface tension and of thermo-mechanical stress fields. Here, the symmetry of the crystal lattices in the two phases is tetragonal and face-centered-cubic in the lead-rich and tin-rich phase, respectively.

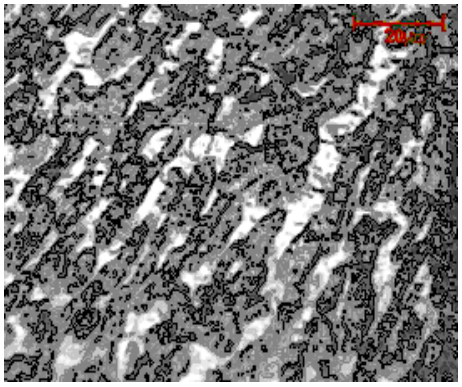

Figure 1: Lead rich (dark) lamellae

We consider coarsening processes that may be subjected to external thermomechanical loads. The given temperature T is assumed to be uniform in space. In this case the morphology and its evolution is described by the fields

$$\begin{aligned} u_i(t,\boldsymbol{X}) \quad &- \quad \text{displacement, leading to the strain } \varepsilon_{ij} = \frac{1}{2}\left(\frac{\partial u_i}{\partial X_j} + \frac{\partial u_j}{\partial X_i}\right), \\ c(t,\boldsymbol{X}) \quad &- \quad \text{mass concentration (e.g. tin),}. \end{aligned} \tag{1.1}$$

Here t denotes the time and $\boldsymbol{X} = (X_1, X_2, X_3)$ are the Lagrange coordinates with respect to a cartesian frame of reference of the material particles of the alloy, which are the smallest volumes units that can be resolved on the considered space scale. The motion of a particle with coordinates $\boldsymbol{X}$ is given by the function $\boldsymbol{x} = \boldsymbol{\chi}(t,\boldsymbol{X})$, which give the actual coordinates $\boldsymbol{x} = (x_1, x_2, x_3)$ of the particle at time t. Its displacement is $u_i = \chi_i - X_i$. The objective of the phase field model is the determination of the fields (1.1). Sometimes it is useful to refer the fields to the actual coordinates. This can be done by the definitions

$$\tilde{c}(t,\boldsymbol{x}) = c(t,\boldsymbol{\chi}^{-1}(t,\boldsymbol{x}))\,, \quad \text{and} \quad \tilde{u}_i(t,\boldsymbol{x}) = u_i(t,\boldsymbol{\chi}^{-1}(t,\boldsymbol{x}))\,. \tag{1.2}$$

The field equations for the displacement and the concentration rely on the quasistatic momentum balance and on the conservation law for the content of one of the two constituents of the binary alloy.

In part I of this study we assume that the displacement field is given, so that we only need the conservation law

$$\rho_0 \frac{\partial c}{\partial t} + \frac{\partial J_k}{\partial X_k} = 0. \tag{1.3}$$

Here, we use the Einstein summation convention which will be frequently used throughout the paper. The constant ρ_0 denotes the mass density of the reference state, which is here given by a homogeneous phase mixture at the eutectic composition, and J_k are the components of the diffusion flux.

The conservation law (1.3) becomes a field equation for the concentration if we relate the diffusion flux to the concentration by a constitutive law that we determine as follows. In the appendix of [5], Dreyer & Müller have exploited the second law of thermodynamics relying on the assumption that the specific free energy, ψ, is given by a function of the type

$$\psi = \hat{\psi}(T, c, \frac{\partial c}{\partial X_i}, \frac{\partial^2 c}{\partial X_i \partial X_j}, \varepsilon_{ij}), \tag{1.4}$$

and they choose Joule/kg as the unit of ψ. In [7] Dreyer & Müller start their reasonings of the form (1.4) on the atomistic scale of a binary alloy in order to derive the function (1.4) explicitely and to exhibit its physical content. In Section 2 of this paper we will give a short survey on the main points of the derivation. Furthermore Dreyer & Müller showed in [5] that in accordance with the second law of thermodynamics, the diffusion flux J_k may be related to the specific free energy by the constitutive law

$$J_k = -\frac{B_{kl}}{T}\frac{\partial \mu}{\partial X_l} \quad \text{with} \quad \mu = \frac{\partial \psi}{\partial c} - \frac{\partial}{\partial X_m}(\frac{\partial \psi}{\partial(\partial c/\partial X_m)}) + \frac{\partial}{\partial X_m \partial X_n}(\frac{\partial^2 \psi}{\partial(\partial^2 c/(\partial X_m \partial X_n))}), \tag{1.5}$$

which generalizes the well known diffusion law according to Fick. The newly introduced quantities B_{kl} are the components of the mobility matrix, which can be related to the matrix of diffusion coefficients.

The idea we pursue in this article is to form the free energy density ψ of the two-phase mixture by interpolation within the interfacial region of the two phases, and use this for the derivation of the diffusion flux for the binary alloy. The resulting model shows that when mechanical effects are neglected the coefficients of the surface tension terms introduce some anisotropy which is due to the concentration dependence of the coefficients. This effect is the main focus of Part I of this study. Hence, here the only field equation will be the diffusion equation. In Part II we will discuss the contributions of mechanical effects to anisotropy.

In the next section we will first begin with a presentation of the Helmholtz free energy, composed of the potential energy between particles and the entropic part and derive expressions for the surface tension coefficients. The corresponding coefficients in the expression for the diffusion flux is then found via the mean field limit In section 3 we use matched asymptotic analysis to derive the corresponding sharp interface model. Interestingly, the expression for the surface tension that results for the sharp interface limit allows only twofold symmetry if mechanical effects are neglected. In section 4 it is shown how the same expression can be found from classical thermodynamics arguments based on the derivation of jump conditions at free boundaries. Finally, in section 5 we derive a boundary integral formulation for the sharp interface model that enables us to employ the non-stiff numerical method, due to [13], for our numerical solution to the problem.

2 Atomistic modeling of phase field systems

2.1 The free energy function for the phase mixture

In this section we establish the constitutive law for the free energy density from an atomistic point of view. To this end we consider separately the two phases, we will call α-phase and β-phase, of the two-phase mixture and calculate at first their individual specific free energy densities ψ_α and ψ_β. In the second step we form the free energy densitiy of the two-phase mixture by interpolation within the interfacial region according to

$$\psi = u\psi_\alpha + (1-u)\psi_\beta, \quad \text{with} \quad u = \begin{cases} 1 & \text{for} \quad \boldsymbol{X} \in \alpha \text{ -phase} \\ 0 & \text{for} \quad \boldsymbol{X} \in \beta \text{ -phase} \end{cases} \tag{2.1}$$

where u is the shape function indicating the phase that occupies the location $\boldsymbol{X}$.

We may relate the shape function to the concentration field by

$$u\left(t, \boldsymbol{X}\right) = \frac{c^\beta\left(T\right) - c\left(t, \boldsymbol{X}\right)}{c^\beta\left(T\right) - c^\alpha\left(T\right)}, \tag{2.2}$$

where $c^\alpha\left(T\right)$ and $c^\beta\left(T\right)$ refer to the equilibrium concentration of the α -phase and β -phase, respectively. Thus the shape function may change continuously in the interfacial region from 0 to 1. There remains the derivation of the free energy functions ψ_α and ψ_β for the individual phases.

2.2 The free energy functions for the individual phases α and β

We consider a body that consists exclusively of the pure phase γ, where γ may generically represent the phase α or β, respectively. The body consists of a crystal lattice, whose symmetry is given, and the lattice sites are randomly occupied by A-type and B-type atoms. We decompose the total free energy of the body into its energetic and its entropic part and write

$$\Psi_\gamma = U_\gamma - TS_\gamma. \tag{2.3}$$

U_γ and S_γ denote the internal energy and the entropy of the body, which now will be determined successively.

The internal energy can be decomposed into a thermal part, $U_\gamma(T)$, which does not interest us at this point, and the potential part, U_{pot}, which is due to the interaction energy between all particles. For simplicity, we assume central forces to act between the atoms a and b, $\{a,b\} \in \{1,2,...N\}$, and we write

$$U_{\gamma|pot} = \Phi_\gamma(x_i^1,...,x_i^N) = \frac{1}{2}\sum_{a,b}\varphi_\gamma^{ab}(r^{ab}) \quad \text{with} \quad r^{ab} = |x^b - x^a|. \tag{2.4}$$

where the 3N-tupel $(x_i^1,...,x_i^N)$ contains the current positions of the atoms. While central force potentials are best suited to explore the key ideas and the atomistic origin of the various contributions appearing in the diffusion flux of phase field models, we note that they are in general not appropriate to describe the behaviour of crystal lattices and may lead to some unrealistic results such as the so-called Cauchy paradox, [14]. In [6] some of the resulting shortcomings are discussed and in [7] this approach has been generalized by using EAM potentials, so that realistic properties of the constitutive law for the diffusion flux are reproduced.

We introduce the microscopic displacements

$$\xi_i^a = x_i^a - X_i^a \tag{2.5}$$

in order to substitute the current positions by the Lagrange positions of the atoms. These substitutions take care of terms up to second order in the displacements, resulting in a linear theory of elasticity.

The case T = 0. In this paragraph we establish the expansion of Φ_γ at $T = 0$. In our derivation we introduce the effects of thermal expansion and other eigenstrains only when taking the mean field limit which simplifies the calculation considerably. The justification for this procedure is given in [14]. At first we obtain from (2.4)

$$U_{\gamma|pot} = \Phi_\gamma(x_i^1,...,x_i^N) = \Phi_\gamma(X_i^1+\xi_i^1,...,X_i^N+\xi_i^N) = \Phi_\gamma(X_i^1,...,X_i^N)+\frac{1}{2}\sum_{a,b}\frac{\partial^2\Phi_\gamma(X_i^1,...,X_i^N)}{\partial X_k^a \partial X_l^b}\xi_k^a\xi_l^b. \tag{2.6}$$

The first derivative does not appear here because at $T = 0$ the potential energy assumes its minimum. Next, we note that there are three different potential functions, viz. φ_γ^{AA} for

$AA-$interactions, φ_γ^{BB} for $BB-$interactions and φ_γ^{AB} for $AB-$interactions. The introduction of the particle concentration operator

$$\hat{y}(a) = \begin{cases} 0 & \text{if} \quad a \text{ indicates an } A \text{ –type atom} \\ 1 & \quad\;\; a \text{ indicates an } B \text{ –type atom} \end{cases}, \tag{2.7}$$

permits us to represent a generic potential φ_γ^{ab} by

$$\varphi_\gamma^{ab} = (1-\hat{y}(a))(1-\hat{y}(b))\varphi_\gamma^{AA} + \hat{y}(a)\hat{y}(b)\varphi_\gamma^{BB} + ((1-\hat{y}(a))\hat{y}(b) + (1-\hat{y}(b))\hat{y}(a))\varphi_\gamma^{AB}. \tag{2.8}$$

This representation will be introduced now in both terms of (2.6). As a consequence herewith there appear new quantities, which are defined as

$$\varphi_\gamma(\Delta^{ab}) = \varphi_\gamma^{AB}(\Delta^{ab}) - \frac{1}{2}(\varphi_\gamma^{AA}(\Delta^{ab}) + \varphi_\gamma^{AB}(\Delta^{ab})), \quad \tilde{\varphi}_\gamma(\Delta^{ab}) = \frac{1}{2}(\varphi_\gamma^{BB}(\Delta^{ab}) - \varphi_\gamma^{AA}(\Delta^{ab})), \tag{2.9}$$

where Δ^{ab} denote the magnitude of the reference distance between atoms a and b. The first sum in equ. (2.6) can now be rewritten as

$$\begin{aligned} &\Phi_\gamma(X_i^1, ..., X_i^N) = \frac{1}{2}\sum_{a,b}\varphi_\gamma^{ab}(\Delta^{ab}) = \\ &\sum_{a,b}(\frac{1}{2}\varphi_\gamma^{AA}(\Delta^{ab}) + \hat{y}(a)(1-\hat{y}(b))\varphi_\gamma(\Delta^{ab}) + \frac{1}{2}(\hat{y}(a)+\hat{y}(b))\tilde{\varphi}_\gamma(\Delta^{ab}), \end{aligned} \tag{2.10}$$

and the second sum in equ. (2.6) results in a simillar manner.

Next we carry out the mean field limit, where quantities that describe the state of an individual atom are replaced by their corresponding mean values and which are assumed to vary slowly in time and space. A detailed discussion on various aspects of the mean field limit are found to be in [10], [14] and [8]. Regarding the atomistic quantities appearing in this paper all authors agree to define the mean field by rules that read

(i) substitute the particle operator, which can only assume the values 0 or 1, by the particle concentration, which may change continuously between 0 and 1:

$$\begin{aligned} &\hat{y}(a) \to y(t, X^a) \equiv y(t, \boldsymbol{X}) \\ &\hat{y}(b) \to y(t, X^a + \Delta^{ab}) \approx y(t, \boldsymbol{X}) + \frac{\partial y(t, \boldsymbol{X})}{\partial X_k}\Delta_k^{ab} + \frac{\partial^2 y(t, \boldsymbol{X})}{\partial X_k \partial X_l}\Delta_k^{ab}\Delta_l^{ab}, \end{aligned} \tag{2.11}$$

and

(ii) substitute the atomic displacement by the mean displacement:

$$\begin{aligned} &\xi_i^a \to u_i(t, X^a) \equiv u_i(t, \boldsymbol{X}) \\ &\xi_i^b \to u_i(t, X^a + \Delta^{ab}) \approx u_i(t, \boldsymbol{X}) + \frac{\partial u_i(t, \boldsymbol{X})}{\partial X_k}\Delta_k^{ab}. \end{aligned} \tag{2.12}$$

Finally we collect all appearing terms and obtain three different contributions to the potential part of the total free energy of the pure phase $\gamma \in \{\alpha, \beta\}$:

$$\begin{aligned} U_{\gamma|pot} = \sum_a \big(& \psi_\gamma^{AA} + \psi_\gamma^{\tilde{\varphi}} y + \psi_\gamma^{\varphi} y(1-y) - \\ & (a_{\gamma|kl}^{\varphi} y - \frac{1}{2} a_{\gamma|kl}^{\tilde{\varphi}} + (A_{\gamma|klmnop}^{\varphi} y - \frac{1}{2} A_{\gamma|klmnop}^{\tilde{\varphi}}) \varepsilon_{mn} \varepsilon_{op}) \frac{\partial^2 y}{\partial X_k \partial X_l} + \\ & \frac{1}{2} (A_{\gamma|mnop}^{AA} + A_{\gamma|mnop}^{\tilde{\varphi}} y + A_{\gamma|mnop}^{\varphi}) \varepsilon_{mn} \varepsilon_{op}). \end{aligned} \tag{2.13}$$

In here, the dependence on the concentration and the strain is explicit and the newly introduced coefficients are constants which can be calculated from the given interaction potentials. Their definitions are given in appendix B. The first line of (2.13) gives the classical local contribution and its third term is the energy of mixing. The first two terms of the second line describes the nonlocal interactions. Its first two terms depend on the concentration and are related to the classical Cahn-Hilliard model, see [1]. Note that first gradients of the atomic concentration, $\partial y / \partial X^k$, do not appear in the representation (2.13) which is due to our restriction to crystal lattices which have either tetragonal or cubic symmetry. Finally, the third line gives the purely elastic part of the potential energy, and the bracket in front of $\varepsilon_{mn}\varepsilon_{op}$ is the stiffness matrix, which, however, turns out to depend concentration.

The case $\mathbf{T > 0}$. For $T > 0$ there results in particular a competition of the energy of mixing and the entropy. In a phase γ with a disordered distribution of the A-type and B-type atoms over the lattice sites, the entropy S_γ is given by

$$S_\gamma = -k \sum_a (y \operatorname{Log}(y) + (1-y) \operatorname{Log}(1-y)). \tag{2.14}$$

Herein k is the Boltzmann constant. If the coefficient ψ_γ^{φ} in (2.13) is positive, the energy of mixing and the entropy may combine so that the local part of the free energy becomes a nonconex function.

Next, we discuss further effects which are induced for $T > 0$. These are eigenstresses as a consequence of eigenstrains, and the most prominent representative is the eigenstrain due to thermal expansion. Other eigenstrains are due to point defects, dislocations and misfit strain. The latter arises for example during phase transitions if the new phase needs more space than the old one. All these effects are described by eigenstrains that have the generic form

$$\varepsilon_{\gamma|mn}^* = \varepsilon_{\gamma|mn}^*(T, c). \tag{2.15}$$

Eigenstrains can be incorporated into the model, i.e into the equation (2.13) by the substitution

$$\varepsilon_{mn} \to (\varepsilon_{mn} - \varepsilon_{\gamma|mn}^*). \tag{2.16}$$

Suppressing its thermal part, we obtain the total free energy for a pure phase γ:

$$\begin{aligned}\Psi_\gamma = \sum_a \big(& \psi^{AA}_\gamma + \psi^{\tilde\varphi}_\gamma y + \psi^{\varphi}_\gamma y(1-y) - \\ & (a^{\varphi}_{\gamma|kl} y - \frac{1}{2} a^{\tilde\varphi}_{\gamma|kl} + (A^{\varphi}_{\gamma|klmnop} y - \frac{1}{2} A^{\tilde\varphi}_{\gamma|klmnop})(\varepsilon_{mn} - \varepsilon^*_{\gamma|mn})(\varepsilon_{op} - \varepsilon^*_{\gamma|op})) \frac{\partial^2 y}{\partial X_k \partial X_l} + \\ & \frac{1}{2}(A^{AA}_{\gamma|mnop} + A^{\tilde\varphi}_{\gamma|mnop} y + A^{\varphi}_{\gamma|mnop})(\varepsilon_{mn} - \varepsilon^*_{\gamma|mn})(\varepsilon_{op} - \varepsilon^*_{\gamma|op}) + \\ & kT \sum_a (y \,\mathrm{Log}(y) + (1-y)\,\mathrm{Log}(1-y))\big).\end{aligned} \tag{2.17}$$

Recall that we need to know the free energy as a function of the mass concentration c rather than a function on the particle concentration y. Both quantities are related to each other by the equation

$$y = \frac{M_A c}{M_B - (M_B - M_A)c}, \tag{2.18}$$

where M_A and M_B are the molecular weights of the constituents A and B, respectively.

2.3 The specific free energy and the diffusion flux of the phase mixture

In (2.17) we may read off the specific free energy ψ_γ of the pure generic phase γ. We consider one mole, and abbreviate each term of the sum in (2.17) by $\tilde\psi_{\gamma|a}$, with $\psi_\gamma = N_A/M(c)\ \tilde\psi_{\gamma|a}$, where $N_A = 6.023 \times 10^{23}$ particles/mole is the Avogadro number. We recall the interpolation (2.1) and obtain the specific free energy of the phase mixture, viz.

$$\psi = \frac{N_A}{M(c)} \left(u(c) \tilde\psi_{\alpha|a} + (1 - u(c)) \tilde\psi_{\beta|a} \right) , \tag{2.19}$$

where

$$M(c) = \frac{M_A M_B}{M_B - (M_B - M_A)c}, \tag{2.20}$$

is the mean molecular weight of the binary mixture. There results a function of the type

$$\psi = \psi_0(c, \varepsilon_{rs}) - a_{jl}(c, \varepsilon_{rs}) \frac{\partial^2 c}{\partial X_j \partial X_l} + b_{jl}(c, \varepsilon_{rs}) \frac{\partial c}{\partial X_j} \frac{\partial c}{\partial X_l}. \tag{2.21}$$

The identification of the local part of the specific free energy ψ_0 and the matrix functions a_{jl} and b_{jl} is done after carrying out the necessary differentiations in order to transfer the y dependent functions $\tilde\psi_{\alpha|a}$ and $\tilde\psi_{\beta|a}$ into functions of the mass concentration c. This calculation is easy but lengthy and left to the interested reader.

Finally, we use the constitutive law (2.1) for the calulation of the diffusion flux. We abbreviate $A_{jl} = a_{jl} + b_{jl}$ and obtain an expression of the following type

$$\begin{aligned} J_k = - \frac{B_{ki}}{T} \frac{\partial}{\partial X_i} \Bigg(& \frac{\partial \psi_0(c, \varepsilon_{rs})}{\partial c} - 2 A_{jl}(c, \varepsilon_{rs}) \frac{\partial^2 c}{\partial X_j \partial X_l} - \frac{\partial A_{jl}(c, \varepsilon_{rs})}{\partial c} \frac{\partial c}{\partial X_j} \frac{\partial c}{\partial X_l} \\ & - 2 \frac{\partial A_{jl}(c, \varepsilon_{rs})}{\partial \varepsilon_{mn}} \frac{\partial c}{\partial X_j} \frac{\partial \varepsilon_{mn}}{\partial X_l} - \frac{\partial^2 a_{jl}(c, \varepsilon_{rs})}{\partial \varepsilon_{mn} \partial \varepsilon_{op}} \frac{\partial \varepsilon_{op}}{\partial X_j} \frac{\partial \varepsilon_{mn}}{\partial X_l} - \frac{\partial a_{jl}(c, \varepsilon_{rs})}{\partial \varepsilon_{mn}} \frac{\partial^2 \varepsilon_{mn}}{\partial X_j \partial X_l} \Bigg) \end{aligned} \tag{2.22}$$

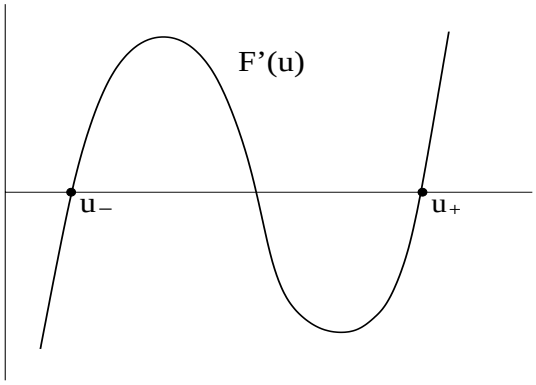

Figure 2:

3 Sharp-Interface limit

For the rest of this study we neglect all mechanical effects. Thus the Lagrange coordinates coincide with the actual coordinates $\boldsymbol{x}$. Furthemore we assume the mobility matrix and temperature to be given constants and $B_{ki} = B\delta_{ki}$. We substitute the resulting expression for the diffusion flux into the conservation equation (1.3) and transform the the equation to the shape function variable $u(t, \boldsymbol{x})$. We nondimensionalize via

$$x_i = L\tilde{x}_i \qquad t = \omega\tilde{t} \qquad \psi = \bar{\psi}\, F(u)\,, \tag{3.1}$$

and obtain after dropping the ' ~ ' for the governing equation

$$u_t = \triangle \mu\,, \tag{3.2}$$

where

$$\mu \;=\; F'(u) - \varepsilon^2 \left(2\, A_{kl}(u)\, \frac{\partial^2 u}{\partial x_k \partial x_l} + A'_{kl}(u) \frac{\partial u}{\partial x_k} \frac{\partial u}{\partial x_l} \right) \tag{3.3}$$

in a domain $\Omega = \Omega_+ \cup \Omega_-$ with

$$\varepsilon^2 = \frac{B\omega}{\bar{T}L^2} \qquad \text{and} \qquad \omega = \frac{\bar{T}(c_\beta - c_\alpha)^2}{B\bar{\psi}}\,, \tag{3.4}$$

where $\bar{T}$ is the constant temperature. The gradient energy coefficients $A_{kl}(u)$ are in general nonlinear functions of $u(t, \boldsymbol{x})$, where we abreviated $A_{kl}(c(u))$ by $A_{kl}(u)$ with $c(u) = c^\beta - \left(c^\beta - c^\alpha\right) u(t, \boldsymbol{x})$. Here, ' ′ ' denotes the derivative with respect to u. The free energy $F(u)$ has a form of a double-well potential, see fig. 2. On the boundary $\partial\Omega$

$$\boldsymbol{n} \cdot \boldsymbol{\nabla} \mu = 0\,, \quad \boldsymbol{n} \cdot \boldsymbol{\nabla} u = 0 \quad \text{on} \quad \partial\Omega\,. \tag{3.5}$$

Solutions of this problem reach phase equilibrium after some time of $O(1)$. Near phase equilibrium, a solution has developed an internal boundary layer structure of $O(\varepsilon)$, approaching sharp interfaces Γ_i of the appearing precipitates, as $\varepsilon \to 0$, see fig. 3. The dynamics of the

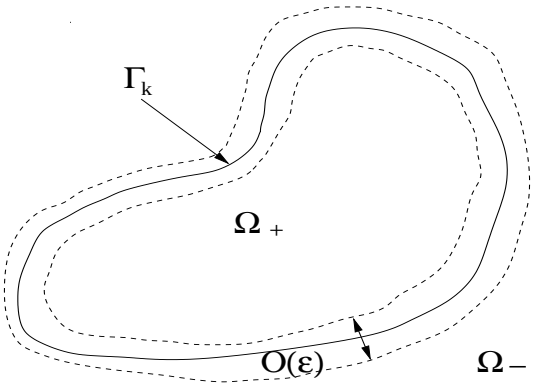

Figure 3: Sketch of sharp interface

precipitates evolves then on the slow time-scale $\tau = \varepsilon t$ and the governing equation describing this is

$$\varepsilon u_\tau = \triangle \mu \tag{3.6}$$

where μ is given by (3.3).

The solution to the corresponding internal boundary layer problem will yield the boundary condition for the "outer problem", i.e. in the region of Ω outside that boundary layer.

3.1 Outer Problem

Let u have the asymptotic expansion

$$u(\tau, \boldsymbol{x}; \varepsilon) = u_{\mathrm{o}}(\tau, \boldsymbol{x}) + \varepsilon u_1(\tau, \boldsymbol{x}) + \varepsilon^2 u_2(\tau, \boldsymbol{x}) + O(\varepsilon^3)\,. \tag{3.7}$$

Correspondingly we can develop μ as

$$\mu(\tau, \boldsymbol{x}; \varepsilon) = \mu_{\mathrm{o}}(\tau, \boldsymbol{x}) + \varepsilon \mu_1(\tau, \boldsymbol{x}) + \varepsilon^2 \mu_2(\tau, \boldsymbol{x}) + O(\varepsilon^3)\,. \tag{3.8}$$

Substitution into (3.2) we obtain together with (3.3) for the leading order problem

$$0 = \triangle \mu_{\mathrm{o}} = \triangle F'(u_{\mathrm{o}})\,. \tag{3.9}$$

The $O(\varepsilon)$ problem is

$$\frac{\partial u_{\mathrm{o}}}{\partial \tau} = \triangle \mu_1 = \triangle \left(F''(u_{\mathrm{o}}) u_1\right)\,, \tag{3.10}$$

and for the $O(\varepsilon^2)$ we obtain

$$\frac{\partial u_1}{\partial \tau} = \triangle \mu_2 = \triangle \left(F''(u_{\mathrm{o}}) u_2 + \frac{1}{2} F'''(u_{\mathrm{o}}) u_1^2 - 2\, A_{kl}(\tilde{u}_{\mathrm{o}})\, \frac{\partial^2 \tilde{u}_{\mathrm{o}}}{\partial x_k \partial x_l} - A'_{kl}(\tilde{u}_{\mathrm{o}}) \frac{\partial \tilde{u}_{\mathrm{o}}}{\partial x_k} \frac{\partial \tilde{u}_{\mathrm{o}}}{\partial X_l} \right) \tag{3.11}$$

plus corresponding boundary conditions on $\partial\Omega$. The boundary conditions on Γ_k will be obtained via matching to the solution of the 'inner' problem valid in the vicinity of the interface Γ_i.

3.2 Inner Problem and Matching

We consider the 2D situation, where $\boldsymbol{x} = (x_1, x_2) = (x, y)$. Let $\boldsymbol{r}(\tau, s) = (r_1(\tau, s), r_2(\tau, s))$ be a parametrization of the curve Γ_k, where s denotes arclength. Then

$$\boldsymbol{x}(\tau, s, z) = \boldsymbol{r}(\tau, s) + \varepsilon\, z\, \boldsymbol{\nu}(\tau, s) \tag{3.12}$$

defines the boundary layer with z being the boundary layer or 'inner' variable, see fig. 4. The normal $\boldsymbol{\nu}(\tau, s) = (-r_{2s}(\tau, s), r_{1s}(\tau, s))$ points inside the precipitate and the tangential $\boldsymbol{t}(\tau, s) = (r_{1s}(\tau, s), r_{2s}(\tau, s))$ points into the counter-clockwise direction.

Making use of appendix A we can expand the gradient energy part in boundary-layer coordinates as follows

$$2\, A_{kl}(u)\, \frac{\partial^2 u}{\partial x_k \partial x_l} + A'_{kl}(u) \frac{\partial u}{\partial x_k} \frac{\partial u}{\partial x_l} = \varepsilon^{-2} g(\tilde{u}, \tilde{u}_{\xi_k}, \tilde{u}_{\xi_k \xi_l}) + \varepsilon^{-1} h(\tilde{u}, \tilde{u}_{\xi_k}, \tilde{u}_{\xi_k \xi_l}) + j(\tilde{u}, \tilde{u}_{\xi_k}, \tilde{u}_{\xi_k \xi_l})\,, \tag{3.13}$$

where $\xi_k,\ \xi_l \in \{s, z\}$ and

$$\begin{aligned}
g(\tilde{u}, \tilde{u}_{\xi_k}, \tilde{u}_{\xi_k \xi_l}) &= 2\, \boldsymbol{\nu} A \boldsymbol{\nu}^\dagger \tilde{u}_{zz} + \boldsymbol{\nu} A' \boldsymbol{\nu}^\dagger \tilde{u}_z^2\,, && (3.14)\\
h(\tilde{u}, \tilde{u}_{\xi_k}, \tilde{u}_{\xi_k \xi_l}) &= -2\, \kappa\, \mathbf{t} A \mathbf{t}^\dagger \tilde{u}_z + 2\, (\mathbf{t} A \boldsymbol{\nu}^\dagger + \boldsymbol{\nu} A \mathbf{t}^\dagger) \tilde{u}_{sz} + (\mathbf{t} A' \boldsymbol{\nu}^\dagger + \boldsymbol{\nu} A' \mathbf{t}^\dagger) \tilde{u}_s \tilde{u}_z\,, && (3.15)\\
j(\tilde{u}, \tilde{u}_{\xi_k}, \tilde{u}_{\xi_k \xi_l}) &= 2\, \mathbf{t} A \mathbf{t}^\dagger \tilde{u}_{ss} + 2\, \kappa\, (\mathbf{t} A' \boldsymbol{\nu}^\dagger + \boldsymbol{\nu} A' \mathbf{t}^\dagger) \tilde{u}_s + \mathbf{t} A \mathbf{t}^\dagger \tilde{u}_s^2 + z\, \kappa\, h(\tilde{u}, \tilde{u}_{\xi_k}, \tilde{u}_{\xi_k \xi_l}) && (3.16)
\end{aligned}$$

with

$$A(\tilde{u}) = \begin{pmatrix} A_{11}(\tilde{u}) & A_{12}(\tilde{u}) \\ A_{21}(\tilde{u}) & A_{22}(\tilde{u}) \end{pmatrix}\,, \tag{3.17}$$

and the superscript † denotes the transpose of a vector. From this we obtain

$$\begin{aligned}
\triangle \mu &= \varepsilon^{-2} \left[F'(\tilde{u}) - g(\tilde{u}, \tilde{u}_{\xi_k}, \tilde{u}_{\xi_k \xi_l})\right]_{zz} - \varepsilon^{-1} \left(h_{zz}(\tilde{u}, \tilde{u}_{\xi_k}, \tilde{u}_{\xi_k \xi_l}) - \kappa \left[F'(\tilde{u}) - g(\tilde{u}, \tilde{u}_{\xi_k}, \tilde{u}_{\xi_k \xi_l})\right]_z\right) \\
&\quad - j_{zz}(\tilde{u}, \tilde{u}_{\xi_k}, \tilde{u}_{\xi_k \xi_l}) - \kappa h_z(\tilde{u}, \tilde{u}_{\xi_k}, \tilde{u}_{\xi_k \xi_l}) + \left[F'(\tilde{u}) - g(\tilde{u}, \tilde{u}_{\xi_k}, \tilde{u}_{\xi_k \xi_l})\right]_{ss} \\
&\quad - z \kappa^2 \left[F'(\tilde{u}) - g(\tilde{u}, \tilde{u}_{\xi_k}, \tilde{u}_{\xi_k \xi_l})\right]_z + O(\varepsilon)
\end{aligned} \tag{3.18}$$

Let the quantities u and μ have the inner expansions

$$\begin{aligned}
\tilde{u}(\tau, s, z) &= \tilde{u}_{\mathrm{o}}(\tau, s, z) + \varepsilon \tilde{u}_1(\tau, s, z) + \varepsilon^2 \tilde{u}_2(\tau, s, z) + O(\varepsilon^3)\,, && (3.19)\\
\tilde{\mu}(\tau, s, z) &= \tilde{\mu}_{\mathrm{o}}(\tau, s, z) + \varepsilon \tilde{\mu}_1(\tau, s, z) + \varepsilon^2 \tilde{\mu}_2(\tau, s, z) + O(\varepsilon^3)\,. && (3.20)
\end{aligned}$$

The function $F(\tilde{u})$ can be expanded as

$$F'(\tilde{u}) = F'(\tilde{u}_{\mathrm{o}}) + \varepsilon\, \tilde{u}_1 F''(\tilde{u}_{\mathrm{o}}) + \varepsilon^2 \left(\frac{1}{2} \tilde{u}_1^2 F'''(\tilde{u}_{\mathrm{o}}) + \tilde{u}_2 F''(\tilde{u}_{\mathrm{o}})\right)\,, \tag{3.21}$$

and $A(\tilde{u})$ can be expanded similarly.

Then, using appendix A and by (3.18) the leading order inner ($O(\varepsilon^{-2})$) problem is

$$\tilde{\mu}_{\mathrm{o}zz} = \left[F'(\tilde{u}_{\mathrm{o}}) - g(\tilde{u}_{\mathrm{o}}, \tilde{u}_{\mathrm{o}\,\xi_k}, \tilde{u}_{\mathrm{o}\,\xi_k \xi_l})\right]_{zz} = 0\,, \tag{3.22}$$

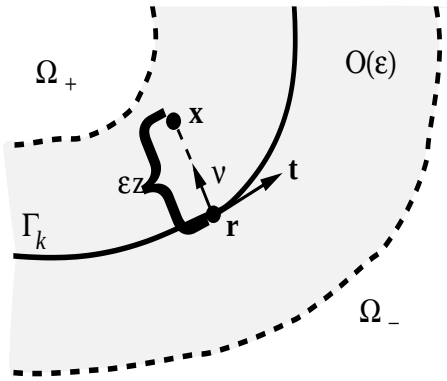

Figure 4: Boundary-layer region

so that

$$\tilde{\mu}_{\rm o}(\tau, \boldsymbol{r}, z) = a_{\rm o}(\tau, \boldsymbol{r})\, z + b_{\rm o}(\tau, \boldsymbol{r})\,. \tag{3.23}$$

Recall that the leading order outer problem for μ is

$$\begin{aligned} \triangle \mu_{\rm o}^- &= 0 \quad \text{in} \quad \Omega^-\,, \\ \boldsymbol{n} \cdot \boldsymbol{\nabla} \mu_{\rm o}^- &= 0 \quad \text{on} \quad \partial\Omega^-\,, \\ \triangle \mu_{\rm o}^+ &= 0 \quad \text{in} \quad \Omega^+\,, \end{aligned} \tag{3.24}$$

where $\mu_{\rm o}^-$ and $\mu_{\rm o}^+$ denote the chemical potential in the matrix and the precipitate, respectively. Both problems have to be joined by a condition on the interface Γ_k of the precipitate. This will be provided by matching with the inner solution. For this we express the outer solution in inner coordinates and reexpand

$$\begin{aligned} &\left(\mu_{\rm o}^\pm + \varepsilon\mu_1^\pm + \varepsilon\mu_2^\pm + O(\varepsilon^3)\right)(\tau, \boldsymbol{r} + \varepsilon z \boldsymbol{\nu}) \\ &= \mu_{\rm o}^\pm(\tau, \boldsymbol{r}) + \varepsilon\left(\mu_1^\pm(\tau, \boldsymbol{r}) + z\, \boldsymbol{\nu} \cdot \boldsymbol{\nabla}_{\boldsymbol{x}}\, \mu_{\rm o}^\pm(\tau, \boldsymbol{r})\right) \\ &\quad + \varepsilon^2 \left(\mu_2^\pm(\tau, \boldsymbol{r}) + z\, \boldsymbol{\nu} \cdot \boldsymbol{\nabla}_{\boldsymbol{x}}\, \mu_1^\pm(\tau, \boldsymbol{r}) + \frac{z^2}{2} \boldsymbol{\nu} H(\mu_{\rm o}^\pm(\tau, \boldsymbol{r}))\boldsymbol{\nu}^T\right) + O(\varepsilon^3)\,, \end{aligned} \tag{3.25}$$

where

$$H(w) := \begin{pmatrix} w_{xx} & w_{xy} \\ w_{yx} & w_{yy} \end{pmatrix}\,. \tag{3.26}$$

Matching to leading order then requires

$$\mu_{\rm o}^\pm(\tau, \boldsymbol{r}) = \lim_{z \to \pm\infty} \tilde{\mu}_{\rm o}(\tau, \boldsymbol{r}, z) \tag{3.27}$$

as $\varepsilon \to 0$. Therefore $a_{\rm o}(\tau, \boldsymbol{r}) = 0$ and $\mu_{\rm o}^\pm(\tau, \boldsymbol{r}) = b_0(\tau, \boldsymbol{r})$.

Furthermore, from the ordinary differential equation for $u_{\rm o}$ in z,

$$\left(2\boldsymbol{\nu} A(\tilde{u}_{\rm o})\boldsymbol{\nu}^\dagger\right)\, \tilde{u}_{{\rm o}\,zz} + \left(\boldsymbol{\nu} A'(\tilde{u}_{\rm o})\boldsymbol{\nu}^\dagger\right)\, \tilde{u}_{{\rm o}\,z}^2 = F'(\tilde{u}_{\rm o}) - b_{\rm o}(\tau, \boldsymbol{r})\,, \tag{3.28}$$

we find

$$\begin{aligned}\frac{1}{2}\frac{d}{dz}\left[\left(2\boldsymbol{\nu}A(\tilde{u}_{\rm o})\boldsymbol{\nu}^{\dagger}\right)\,\tilde{u}_{{\rm o}\,z}^{2}\right] &= \left[\left(2\boldsymbol{\nu}A(\tilde{u}_{\rm o})\boldsymbol{\nu}^{\dagger}\right)\,\tilde{u}_{{\rm o}\,zz}+\left(\boldsymbol{\nu}A'(\tilde{u}_{\rm o})\boldsymbol{\nu}^{\dagger}\right)\,\tilde{u}_{{\rm o}\,z}\right]\,\tilde{u}_{{\rm o}\,z}^{2}\\ &= \left(F'(\tilde{u}_{\rm o})-b_{\rm o}(\tau,\boldsymbol{r})\right)\,\tilde{u}_{{\rm o}\,z}\,. \end{aligned}\tag{3.29}$$

This yields, after we integrate from $z=+\infty$ to $z=-\infty$ and observe that $\tilde{u}_{{\rm o}\,z}\to 0$ as $z\to\pm\infty$, the solvability condition

$$\int_{u_-}^{u^+} F'(\tilde{u}_{\rm o})-b_{\rm o}(\tau,\boldsymbol{r})\,d\tilde{u}_{\rm o}=0\quad\text{with}\quad F'(u^{\pm})=b_{\rm o}\,.\tag{3.30}$$

From phase plane analysis we infer that there is a unique constant $b_{\rm o}$ satisfying (3.30). Finally, the uniqueness of solution to the problem

$$\begin{aligned}\triangle\mu_{\rm o}^{-} &= 0 \quad\text{in}\quad \Omega^{-}\,,\\ \boldsymbol{n}\cdot\boldsymbol{\nabla}\mu_{\rm o}^{-} &= 0 \quad\text{on}\quad \partial\Omega^{-}\,,\\ \mu_{\rm o}^{\pm} &= b_{\rm o}\quad\text{on}\quad \Gamma_k\,,\\ \triangle\mu_{\rm o}^{+} &= 0 \quad\text{in}\quad \Omega^{+}\,,\end{aligned}\tag{3.31}$$

ensures that $\mu_{\rm o}=$ const. in all of Ω.

To order $O(\varepsilon^{-1})$ we obtain for the inner problem

$$\begin{aligned}0 &= -h_{zz}(\tilde{u}_{\rm o},\tilde{u}_{{\rm o}\,\xi_k},\tilde{u}_{{\rm o}\,\xi_k\xi_l})+\kappa\mu_{{\rm o}\,z}+\left[F''(\tilde{u}_{\rm o})\tilde{u}_1-2\boldsymbol{\nu}A(\tilde{u}_{\rm o})\boldsymbol{\nu}^{\dagger}\tilde{u}_{1\,zz}\right.\\ &\quad\left.-2\boldsymbol{\nu}A'(\tilde{u}_{\rm o})\tilde{u}_1\boldsymbol{\nu}^{\dagger}\tilde{u}_{{\rm o}\,zz}-2\boldsymbol{\nu}A'\boldsymbol{\nu}^{\dagger}\tilde{u}_{{\rm o}\,z}\tilde{u}_{1\,z}+\boldsymbol{\nu}A''(\tilde{u}_{\rm o})\tilde{u}_1\boldsymbol{\nu}^{\dagger}\tilde{u}_{{\rm o}\,z}^{2}\right]_{zz}\\ &= -h_{zz}(\tilde{u}_{\rm o},\tilde{u}_{{\rm o}\,\xi_k},\tilde{u}_{{\rm o}\,\xi_k\xi_l})+\kappa\mu_{{\rm o}\,z}+\left[\lim_{\varepsilon\to 0}\frac{d}{d\,\varepsilon}\left(F'(\tilde{u})-g(\tilde{u},\tilde{u}_{\xi_k},\tilde{u}_{\xi_k\xi_l})\right)\right]_{zz}\,.\end{aligned}\tag{3.32}$$

Note, $\tilde{\mu}_{\rm o}$ is constant so that $\kappa\tilde{\mu}_{{\rm o}\,z}=0$ and the right hand side of (3.32) is equal to $\tilde{\mu}_{1\,zz}$. Hence,

$$\tilde{\mu}_1(\tau,\boldsymbol{r},z)=a_1(\tau,\boldsymbol{r})\,z+b_1(\tau,\boldsymbol{r})\,.\tag{3.33}$$

Moreover, since $\mu_{\rm o}$ is constant, matching to next order yields

$$\mu_1^{\pm}(\tau,\boldsymbol{r})=\lim_{z\to\pm\infty}\tilde{\mu}_1(\tau,\boldsymbol{r},z)\,.\tag{3.34}$$

Hence, $a_1(\tau,\boldsymbol{r})=0$ and $\tilde{\mu}_1=b_1(\tau,\boldsymbol{r})$ is independent of z and

$$\tilde{\mu}_1(\tau,\boldsymbol{r})=-h(\tilde{u}_{\rm o},\tilde{u}_{{\rm o}\,\xi_k},\tilde{u}_{{\rm o}\,\xi_k\xi_l})+\lim_{\varepsilon\to 0}\frac{d}{d\varepsilon}\left(F'(\tilde{u})-g(\tilde{u},\tilde{u}_{\xi_k},\tilde{u}_{\xi_k\xi_l})\right)\,.\tag{3.35}$$

Note now, that

$$\begin{aligned}\frac{\partial}{\partial s}\left[\left(\mathbf{t}A\boldsymbol{\nu}^{\dagger}+\boldsymbol{\nu}A\mathbf{t}^{\dagger}\right)\tilde{u}_{{\rm o}\,z}^{2}\right] &= \left(\mathbf{t}A\boldsymbol{\nu}^{\dagger}+\boldsymbol{\nu}A\mathbf{t}^{\dagger}\right)2\tilde{u}_{{\rm o}\,z}\tilde{u}_{{\rm o}\,sz}+\left(\mathbf{t}A'\boldsymbol{\nu}^{\dagger}+\boldsymbol{\nu}A'\boldsymbol{\nu}^{\dagger}\right)\tilde{u}_{{\rm o}\,s}\tilde{u}_{{\rm o}\,z}^{2}\\ &\quad -2\kappa\left(\mathbf{t}A\mathbf{t}^{\dagger}-\boldsymbol{\nu}A\boldsymbol{\nu}^{\dagger}\right)\tilde{u}_{{\rm o}\,z}^{2}\,.\end{aligned}\tag{3.36}$$

This implies

$$\begin{aligned}\tilde{u}_{\mathrm{o}\,z}\,\tilde{\mu}_1(\tau,\boldsymbol{r}) &= 2\,\kappa\,\boldsymbol{\nu}A\boldsymbol{\nu}^\dagger\tilde{u}^2_{\mathrm{o}\,z} - \frac{\partial}{\partial s}\left[\left(\mathbf{t}A\boldsymbol{\nu}^\dagger + \boldsymbol{\nu}A\mathbf{t}^\dagger\right)\tilde{u}^2_{\mathrm{o}\,z}\right]\\ &\quad +\tilde{u}_{\mathrm{o}\,z}\lim_{\varepsilon\to 0}\frac{d}{d\varepsilon}\left(F'(\tilde{u}) - g(\tilde{u},\tilde{u}_{\xi_k},\tilde{u}_{\xi_k\xi_l})\right)\,. \end{aligned} \tag{3.37}$$

The condition joining the two outer problems for μ_1 is obtained now by integrating (3.37) from $z=-\infty$ to $z=+\infty$. First we observe that the third term on the right hand side vanishes. For this recall that

$$\begin{aligned}\tilde{u}_{\mathrm{o}\,z}\lim_{\varepsilon\to 0}\frac{d}{d\varepsilon}\left(F'(\tilde{u}) - g(\tilde{u},\tilde{u}_{\xi_k},\tilde{u}_{\xi_k\xi_l})\right) &= F''(\tilde{u}_{\mathrm{o}})\tilde{u}_{\mathrm{o}\,z}\tilde{u}_1 - 2\boldsymbol{\nu}A\boldsymbol{\nu}^\dagger\tilde{u}_{1\,zz}\tilde{u}_{\mathrm{o}\,z} - \boldsymbol{\nu}A''\boldsymbol{\nu}^\dagger\tilde{u}_1\tilde{u}^3_{\mathrm{o}\,z}\\ &\quad -2\boldsymbol{\nu}A'\boldsymbol{\nu}^\dagger\tilde{u}^2_{\mathrm{o}\,z}\tilde{u}_{1\,z} - 2\boldsymbol{\nu}A'\boldsymbol{\nu}^\dagger\tilde{u}_1\tilde{u}_{\mathrm{o}\,z}\tilde{u}_{\mathrm{o}\,zz} \end{aligned} \tag{3.38}$$

and note that (3.28) implies

$$\begin{aligned}F''(\tilde{u}_{\mathrm{o}})\tilde{u}_{\mathrm{o}\,z}\tilde{u}_1 &= 2\boldsymbol{\nu}A'\boldsymbol{\nu}^\dagger\tilde{u}_1\tilde{u}_{\mathrm{o}\,z}\tilde{u}_{\mathrm{o}\,zz} + 2\boldsymbol{\nu}A\boldsymbol{\nu}^\dagger\tilde{u}_1\tilde{u}_{\mathrm{o}\,zzz}\\ &\quad +\boldsymbol{\nu}A''\boldsymbol{\nu}^\dagger\tilde{u}_1\tilde{u}^3_{\mathrm{o}\,z} + 2\boldsymbol{\nu}A'\boldsymbol{\nu}^\dagger\tilde{u}_1\tilde{u}_{\mathrm{o}\,z}\tilde{u}_{\mathrm{o}\,zz}\,. \end{aligned} \tag{3.39}$$

Hence

$$\tilde{u}_{\mathrm{o}\,z}\lim_{\varepsilon\to 0}\frac{d}{d\varepsilon}\left(F'(\tilde{u}) - g(\tilde{u},\tilde{u}_{\xi_k},\tilde{u}_{\xi_k\xi_l})\right) = \left[2\boldsymbol{\nu}A\boldsymbol{\nu}^\dagger\left(\tilde{u}_1\tilde{u}_{\mathrm{o}\,zz} - \tilde{u}_{1\,z}\tilde{u}_{\mathrm{o}\,z}\right)\right]_z \tag{3.40}$$

the integral over which from $z=-\infty$ to $z=+\infty$ vanishes since $\tilde{u}_{\mathrm{o}\,z}$, $\tilde{u}_{\mathrm{o}\,zz}\to 0$ for $z\to\pm\infty$. For the integral of the two other terms on the right hand side, we define

$$G(\tilde{u}_{\mathrm{o}}) = \int_{u_-}^{\tilde{u}_{\mathrm{o}}} F'(v) - b_{\mathrm{o}}\,dv \tag{3.41}$$

and observe that from (3.28)

$$\tilde{u}_{\mathrm{o}\,z} = \sqrt{\frac{G(\tilde{u}_{\mathrm{o}})}{\boldsymbol{\nu}A\boldsymbol{\nu}^\dagger}} \tag{3.42}$$

so that the integral of (3.37) can be written

$$[u^\pm]\,\tilde{\mu}_1(\tau,\boldsymbol{r}) = 2\kappa\int_{u_-}^{u^+}\sqrt{\boldsymbol{\nu}A\boldsymbol{\nu}^\dagger G(v)}\,dv - \frac{\partial}{\partial s}\int_{u_-}^{u^+}\left(\mathbf{t}A\boldsymbol{\nu}^\dagger + \boldsymbol{\nu}A\mathbf{t}^\dagger\right)\sqrt{\frac{G(v)}{\boldsymbol{\nu}A\boldsymbol{\nu}^\dagger}}\,dv \tag{3.43}$$

This can also be written, after differentiation with respect to s, as

$$\tilde{\mu}_1(\tau,\boldsymbol{r}) = \frac{\kappa}{[u^\pm]}\left(2\int_{u_-}^{u^+}\mathbf{t}A\mathbf{t}^\dagger\sqrt{\frac{G(v)}{\boldsymbol{\nu}A\boldsymbol{\nu}^\dagger}}\,dv - \frac{1}{2}\int_{u_-}^{u^+}\left(\mathbf{t}A\boldsymbol{\nu}^\dagger + \boldsymbol{\nu}A\mathbf{t}^\dagger\right)^2\sqrt{\frac{G(v)}{(\boldsymbol{\nu}A\boldsymbol{\nu}^\dagger)^3}}\,dv\right)\,. \tag{3.44}$$

By the matching condition (3.34) this equals $\mu_1(\tau,\boldsymbol{r})$. Given $F(u)$ and $A(u)$ it represents the chemical potential along the interface Γ_k of a precipitate. This leads to the sharp interface model

$$\begin{aligned}\triangle\mu_1^- &= 0 \quad \text{in} \quad \Omega^-\,, &(3.45)\\ \boldsymbol{n}\cdot\boldsymbol{\nabla}\mu_1^- &= 0 \quad \text{on} \quad \partial\Omega^-\,, &(3.46)\\ \mu_1^\pm &= \tilde{\mu}_1(\tau,\boldsymbol{r})\,, &(3.47)\\ \triangle\mu_1^+ &= 0 \quad \text{in} \quad \Omega^+\,. &(3.48)\end{aligned}$$

In order to determine the velocity of the sharp interface we have to continue the matching to higher order. To order $O(1)$ the inner problem reads

$$\begin{aligned} -V^{\boldsymbol{\nu}}\tilde{u}_{\mathrm{o}\,z} &= -j_{zz}(\tilde{u}_{\mathrm{o}},\tilde{u}_{\mathrm{o}\,\xi_k},\tilde{u}_{\mathrm{o}\,\xi_k\xi_l}) - \kappa h_z(\tilde{u}_{\mathrm{o}},\tilde{u}_{\mathrm{o}\,\xi_k},\tilde{u}_{\mathrm{o}\,\xi_k\xi_l}) + \mu_{\mathrm{o}\,ss} - z\kappa\mu_{\mathrm{o}\,z} \\ &\quad - \lim_{\varepsilon\to 0}\frac{d}{d\,\varepsilon}\left(h_{zz}(\tilde{u},\tilde{u}_{\xi_k},\tilde{u}_{\xi_k\xi_l}) - \kappa\left[F'(\tilde{u})-g(\tilde{u})\right]_z\right) + \lim_{\varepsilon\to 0}\frac{d^2}{d\,\varepsilon^2}\left[F'(\tilde{u})-g(\tilde{u})\right]_{zz}\,, \end{aligned} \tag{3.49}$$

where $V^{\boldsymbol{\nu}} = \boldsymbol{x}_\tau\cdot\boldsymbol{\nu}$. Again, since μ_{o} is constant, we have

$$\begin{aligned} -V^{\boldsymbol{\nu}}\tilde{u}_{\mathrm{o}\,z} &= \tilde{\mu}_{2\,zz} - \kappa\left[h(\tilde{u}_{\mathrm{o}},\tilde{u}_{\mathrm{o}\,\xi_k},\tilde{u}_{\mathrm{o}\,\xi_k\xi_l}) - \lim_{\varepsilon\to 0}\frac{d}{d\,\varepsilon}\left(F'(\tilde{u})-g(\tilde{u},\tilde{u}_{\xi_k},\tilde{u}_{\xi_k\xi_l})\right)\right]_z \\ &= \tilde{\mu}_{2\,zz} - \kappa\tilde{\mu}_{1\,z}\,. \end{aligned} \tag{3.50}$$

Since $\tilde{\mu}_1$ is independent of z, we simply have

$$-V^{\boldsymbol{\nu}}\tilde{u}_{\mathrm{o}\,z} = \tilde{\mu}_{2\,zz}\,. \tag{3.51}$$

We integrate (3.51) once with respect to z and use the matching condition for $\tilde{\mu}_{2\,z}$ to obtain for $z\to\pm\infty$

$$\lim_{z\to\pm\infty}\tilde{\mu}_{2\,z} = \boldsymbol{\nu}\cdot\boldsymbol{\nabla}_x\mu_1^{\pm}(\tau,\boldsymbol{r})\,. \tag{3.52}$$

The z^2-term in (3.25) vanishes since μ_{o} is constant. Hence, we obtain for the interfacial speed

$$V^{\boldsymbol{\nu}} = -\frac{[\boldsymbol{\nu}\cdot\boldsymbol{\nabla}_x\mu_1^{\pm}(\tau,\boldsymbol{r})]}{[u^{\pm}]} \tag{3.53}$$

3.3 The Cahn-Hoffmann law for concentration dependent surface energy

We also obtain for a concentration dependent surface energy a Cahn-Hoffmann law, [2], [3], [11]. To this end we define

$$\boldsymbol{r}_s = (\cos\theta(\tau,s),\,\sin\theta(\tau,s))\,, \tag{3.54}$$

where $\theta(\tau,s)$ is the angle of the tangent at a point on Γ_k to the x-axis. In terms of this coordinate we have

$$\left(\boldsymbol{\nu}A\boldsymbol{\nu}^\dagger\right)_{\theta\theta} = 2\left(\mathbf{t}A\mathbf{t}^\dagger - \boldsymbol{\nu}A\boldsymbol{\nu}^\dagger\right)\,. \tag{3.55}$$

Using this we can derive

$$2\left(\sqrt{(\boldsymbol{\nu}A\boldsymbol{\nu}^\dagger)_{\theta\theta}} + \sqrt{(\boldsymbol{\nu}A\boldsymbol{\nu}^\dagger)}\right) = 2\frac{\mathbf{t}A\mathbf{t}^\dagger}{\sqrt{\boldsymbol{\nu}A\boldsymbol{\nu}^\dagger}} - \frac{1}{2}\frac{\left(\mathbf{t}A\boldsymbol{\nu}^\dagger + \boldsymbol{\nu}A\mathbf{t}^\dagger\right)^2}{\left(\boldsymbol{\nu}A\boldsymbol{\nu}^\dagger\right)^{-3/2}}\,, \tag{3.56}$$

so that

$$\mu_1(\tau,\boldsymbol{r}) = \frac{\kappa}{[u^{\pm}]}\left(\sigma+\sigma_{\theta\theta}\right)\,, \tag{3.57}$$

where the surface tension σ is defined as

$$\sigma = 2\int_{u_-}^{u^+}\sqrt{\boldsymbol{\nu}A\boldsymbol{\nu}^\dagger G(v)}\,dv\,. \tag{3.58}$$

At this point it is interesting to observe that the expression for the surface tension σ allows at most two-fold symmetry. This is in contrast to previous theories, e.g. [12] etc., where it was assumed that the surface tension reflects the symmetry of the underlying crystal lattice and could in principle have higher symmetry. Our analysis shows that in fact higher symmetries of the surface tension enter only through mechanical effects, which is shown in Part II of this study.

3.4 Generalization to 3D

The sharp interface limit implies in first and second order the conditions (3.30) and (3.43), respectively. The condition (3.30) yields the equilibrium concentrations according to the common tangent construction, which describes the jump conditions if the curvature of the interface is ignored. The condition (3.43) takes care of curvature and yields the corrections to the plane interface case. Up to now we considered exclusively a phase mixture in 2D with interfaces as 1D objects. While the common tangent construction is not influenced by this restriction, the condition (3.43) is. A generalization to the case of a phase mixture in 3D with interfaces as 2D surfaces can be carried out along similar strategies. In this case the interfaces are described by two Gaussian parameters U^Δ, $\Delta \in \{1,2\}$ and the function $\boldsymbol{r}(\tau, U^1, U^2)$ gives the location of the surface points. The surface is equipped with a unit normal $\boldsymbol{\nu}$, two tangent vectors $\boldsymbol{t}_\Delta$, a metric, $g_{\Delta\Gamma}$, and a Gaussian curvature tensor, $b_{\Delta\Gamma}$. The mean curvature is defined by $\kappa_M = (1/2)\, g^{\Delta\Gamma} b_{\Delta\Gamma}$. All these quantities can be calulated from the surface function $\boldsymbol{r}(\tau, U^1, U^2)$.

The corresponding expression to (3.43) reads

$$[u^\pm]\mu_1 = 2\sigma\kappa_M + (-\frac{1}{2}\sigma^\Delta)_{;\Delta}, \tag{3.59}$$

where the semicolon indicates the covariant derivative, and with

$$\sigma = 2\int_{u^-}^{u^+} \sqrt{\boldsymbol{\nu} A \boldsymbol{\nu}^\dagger G(v)}\, dv, \quad \sigma_\Delta = 2\int_{u^-}^{u^+} (\boldsymbol{\nu} A \mathbf{t}_\Delta^\dagger + \mathbf{t}_\Delta A \boldsymbol{\nu}^\dagger)\sqrt{\frac{G(v)}{\boldsymbol{\nu} A \boldsymbol{\nu}^\dagger}}\, dv. \tag{3.60}$$

4 Jump conditions for a binary mixture according to classical thermodynamics

The sharp interface limit from section 3 reveals jump conditions at the interface between the two coexisting phases. Jump conditions, however, can also be obtained from classical thermodynamics that models the interfaces from the very beginning on as singular surfaces [9]. Here, we consider classical thermodynamics of a binary disordered mixture that may consist of two coexisting phases α and β, and we ignore mechanical stress fields in the bulk. In this case the variables are the temperature T and the partial mass densities ρ^A and ρ^B of the two

constituents A and B. The specific free energy density is given by a function of the type

$$\psi = \hat{\psi}(T, \rho^A, \rho^B), \quad \text{and} \quad \mu^A = \frac{\partial \rho \hat{\psi}}{\partial \rho^A} \quad \text{and} \quad \mu^B = \frac{\partial \rho \hat{\psi}}{\partial \rho^B} \tag{4.1}$$

are the chemical potentials of the constituents, see e.g. [17]. Herein $\rho = \rho^A + \rho^B$ denotes the mass density of the mixture.

It is useful to change the variables ρ_A, ρ_B according to

$$(\rho^A, \rho^B) \to (\rho, c = \rho^B/\rho) \tag{4.2}$$

We write

$$\hat{\psi}(T, \rho^A, \rho^B) = \tilde{\psi}(T, \rho, c), \quad \text{and} \quad p = \rho^2 \frac{\partial \rho \tilde{\psi}}{\partial \rho} \tag{4.3}$$

defines the pressure. Next we calculate the chemical potentials from the function $\tilde{\psi}$. There results

$$\mu^A = \psi + \frac{p}{\rho} - c\tilde{\psi}' \quad \text{and} \quad \mu^B = \psi + \frac{p}{\rho} + (1-c)\tilde{\psi}' \quad \text{with} \quad \tilde{\psi}' = \frac{\partial \tilde{\psi}}{\partial c}. \tag{4.4}$$

Note that there holds

$$\mu \equiv \mu^B - \mu^A = \tilde{\psi}'. \tag{4.5}$$

The jump conditions at the interface are derived in classical thermodynamics by means of generic balance equations [9]. Denoting the limits of a generic quantity g that approach the interface from the α-phase and β-phase, respectively, by g_α and g_β, the jump conditions read

$$\mu^A_\beta - \mu^A_\alpha = 0, \quad \mu^B_\beta - \mu^B_\alpha = 0 \quad \text{and} \quad p_\beta - p_\alpha = S^{\Delta\Gamma} b_{\Delta\Gamma} + S^{\Delta}_{;\Delta}. \tag{4.6}$$

The newly introduced quantities are the tangential surface stress, $S^{\Delta\Gamma}$, the normal surface stress, S^{Δ}, and the semicolon indicates the covariant derivative.

Thermodynamics of interfaces relates the surface stresses $S^{\Delta\Gamma}$and S^{Δ} to the free energy density, ψ_s, of the interface. Under the assumptions, that

$$\text{(i) } T_\beta = T_\alpha \equiv T, \qquad \text{(ii) } \psi_s \text{ may depend on } T,\ \nu^i \text{ and } g_{\Delta\Gamma}$$

there holds as a consequence of the second law of thermodynamics

$$S^{\Delta\Gamma} = \psi_s g^{\Delta\Gamma} + \frac{1}{2}\frac{\partial \psi_s}{\partial g_{\Delta\Gamma}} \quad \text{and} \quad S^{\Delta} = -g^{\Delta\Gamma}\tau^i_\Gamma \frac{\partial \psi_s}{\partial \nu^i}, \tag{4.7}$$

see [9] for details. The first contribution of $S^{\Delta\Gamma}$ leads in $(4.6)_3$ to the classical capillary force which is proportional to the mean curvature $\kappa_M = (1/2)\, g^{\Delta\Gamma} b_{\Delta\Gamma}$. The metric dependence of the interfacial free energy describes elastic effects of the interface and the normal surface stress, given by $(4.7)_2$ which is related to the Hoffmann-Cahn vector.

Next we will evaluate the jump condition (4.6). At first we write the conditions $(4.6)_{1,2}$ more explicit:

$$\tilde{\psi}'_\beta(T, \rho_\beta, c_\beta) = \tilde{\psi}'_\alpha(T, \rho_\alpha, c_\alpha) \equiv \mu \quad \text{and} \quad (c_\beta - c_\alpha)\mu = \tilde{\psi}_\beta - \tilde{\psi}_\alpha + \frac{p_\beta}{\rho_\beta} - \frac{p_\alpha}{\rho_\alpha}. \tag{4.8}$$

Let us assume for simplicity $\rho_\beta \approx \rho_\alpha \equiv \rho$, and let $c_{\beta\,0}$, $c_{\alpha\,0}$ be the solution of

$$\tilde{\psi}'_\beta(T,\rho,c_\beta) = \tilde{\psi}'_\alpha(T,\rho,c_\alpha) \quad \text{and} \quad (c_\beta - c_\alpha)\mu = \tilde{\psi}_\beta - \tilde{\psi}_\alpha, \tag{4.9}$$

which describes the common tangent construction, also called Maxwell construction. We conclude that the common tangent construction only holds if

$$\text{(i) } p_\beta = p_\alpha \equiv p_0 \qquad \text{and} \qquad \text{(ii) } \rho_\beta = \rho_\alpha \equiv \rho_0.$$

Note at this point that condition (i) is well-known, but the necessity of the second condition is in general not noted. In the following we will take the condition (ii) for granted. Note that in the derivation of the sharp interface limit from the reduced phase field model we also did not consider the variation of the total density of the binary mixture. Furthermore, note that this variation is related to the trace of the mechanical strain, which will be included in Part II of this study.

We proceed to exploit the jump conditions (4.6). To this end we make the Ansatz

$$c_\alpha = c_{\alpha\,0} + c_{\alpha\,1}, \quad c_\beta = c_{\beta\,0} + c_{\beta\,1}, \quad p_\alpha = p_{\alpha\,0} + p_{\alpha\,1}, \quad p_\beta = p_{\beta\,0} + p_{\beta\,1}, \quad \mu = \mu_0 + \mu_1 \tag{4.10}$$

and exploit the jump condition $(4.8)_1$ under the assumption that quantities with index 1 are small corrections to the corresponding quantities with index 0. There results

$$\mu_0 = \tilde{\psi}'_\alpha(T,\rho_0,c_{\alpha\,0}) = \tilde{\psi}'_\beta(T,\rho_0,c_{\beta\,0}), \quad \mu_1 = \tilde{\psi}''_\alpha(T,\rho_0,c_{\alpha\,0})c_{\alpha\,1} = \tilde{\psi}''_\beta(T,\rho_0,c_{\beta\,0})c_{\beta\,1}, \tag{4.11}$$

while the conditions $(4.8)_2$ and $(4.6)_2$ imply

$$(c_{\beta\,0} - c_{\alpha\,0})\mu_1 = \frac{1}{\rho_0}(S^{\Delta\Gamma}b_{\Delta\Gamma} + S^{\Delta}_{;\Delta}). \tag{4.12}$$

Let us now ignore elastic effects of the interface so that the right hand side of (4.12) can be rewritten as

$$(c_{\beta\,0} - c_{\alpha\,0})\mu_1 = \frac{1}{\rho_0}(2\psi_s\kappa_M + (-g^{\Delta\Gamma}\tau^i_\Gamma\frac{\partial\psi_s}{\partial\nu^i})_{;\Delta}). \tag{4.13}$$

A comparison of (4.13) with the corresponding result (3.59), that we have obtained from the phase field model, suggests to identifiy

$$\psi_s = \sigma. \tag{4.14}$$

In this case the definitions (3.60) imply that the interfacial free energy density has the following properties

$$\nu^i\frac{\partial\psi_s}{\partial\nu^i} = \psi_s \quad \text{and} \quad \tau^i_\Delta\frac{\partial\psi_s}{\partial\nu^i} = \frac{1}{2}\sigma_\Delta. \tag{4.15}$$

The result (4.13) of classical thermodynamics can thus be written

$$\rho_{\rm o}(c_{\beta\,0} - c_{\alpha\,0})\mu_1 = 2\sigma\kappa_M + (-\frac{1}{2}\sigma^\Delta)_{;\Delta}\,. \tag{4.16}$$

This resultis in agreement with (3.59) developed from the phase field model.

5 Numerical methods

For our numerical treatment we follow [12] and transform the sharp interface model (3.45)–(3.48), (3.53) into a boundary integral formulation. Note, that the sharp interface model describes mass diffusion in the matrix and mass diffusion in the precipitates connected by the common boundary condition (3.47). Here, we make the simplifying assumption that diffusion in the precipitates can be neglected, i.e. we treat only the one-sided model

$$\begin{aligned} \triangle \mu_1^- &= 0 \quad \text{in} \quad \Omega^- && (5.1)\\ \boldsymbol{n} \cdot \boldsymbol{\nabla} \mu_1^- &= 0 \quad \text{on} \quad \partial\Omega^- && (5.2)\\ \mu_1^- &= \tilde{\mu}_1 \quad \text{on} \quad \Gamma && (5.3) \end{aligned}$$

and

$$[u^{\pm}]\, V^{\boldsymbol{\nu}} = \boldsymbol{\nu} \cdot \boldsymbol{\nabla} \mu_1^- \qquad \text{on } \Gamma \tag{5.4}$$

and drop the superscript $(-)$ from now on. We further assume that $\partial\Omega$ has been shifted to infinity and replace the local condition

$$\boldsymbol{n} \cdot \boldsymbol{\nabla} \mu_1 = 0 \;\text{ by the condition of no flux in the far field }\; \lim_{R_\infty \to \infty} \int n \cdot \boldsymbol{\nabla} \mu_1 = 0\,. \tag{5.5}$$

In what follows, we note that the tangential vector $\boldsymbol{t}$ to the boundary of a precipitate always points into the mathematically positive direction, and $\boldsymbol{\nu}$ always points to the left, i.e. inside the precipitate.

We want a boundary integral representation for the solution of

$$\begin{aligned} \triangle \mu_1 &= 0 \qquad \text{in } \Omega_- \\ \text{by setting} \quad \mu_1 &= \text{Re}\,(\Psi(z)) \quad z = x + iy\,, z \in \Omega_- \end{aligned} \tag{5.6}$$

where

$$\Psi(z) = \sum_{k=1}^{N} A_k \ln(z - M_k) + \frac{1}{2\pi i} \int_\Gamma \frac{\Phi(\zeta)}{\zeta - z} d\zeta + \frac{1}{2\pi} \int \Phi(\zeta) d\zeta \tag{5.7}$$

where $A_k \in \mathbb{R}$, $\Phi \in \mathbb{C}$ and the complex number $M_k \in \Omega_k$, being the interior of Γ_k, where $\Gamma := \bigcup_{k=1}^{N} \Gamma_k$. The first term on the r.h.s. represents the contribution of the 2D-precipitates, the second term is the analytical part for $z \in \Omega_-$ and the third part is a constant correction if $\Psi \not\to 0$ for $z \to \infty$. As has been shown by Mikhlin [16] this representation is unique for given z_k. Furthermore, it is shown in [16], that for $z \to \tilde{z} \in \Gamma$

$$\begin{aligned} \text{Re}\left(\lim_{\substack{z \to \tilde{z} \\ z \in \Omega_-}} \Psi \right) &= -\frac{1}{2}\Phi(\tilde{z}) + \sum_{k=1}^{N} A_k \ln(\tilde{z} - M_k) + \frac{1}{2\pi} \Im \int_\Gamma \frac{\Phi(\zeta)}{\zeta - z} d\zeta + \frac{1}{2\pi} \int \Phi(\zeta) d\zeta \\ &= \mu_1|_\Gamma \end{aligned} \tag{5.8}$$

i.e. for μ_1 on Γ . Substitution of (5.6), (5.7) into (5.5) yields

$$\sum_{k=1}^{N} A_k = 0\,. \tag{5.9}$$

Note, that the l.h.s. of (5.8) is an integral operator on Φ with kernel of dim $= N-1$ so that we have $N-1$ solvability conditions for the r.h.s. of (5.8). Together with (5.9) this will fix the A_k, so that we can find the corresponding Φ. In order to obtain uniqueness one has to impose the constraints (see again [16])

$$\int_{\Gamma_k} \Phi(\zeta)\, d\zeta = 0. \tag{5.10}$$

Now we can determine μ_1 on Γ and hence $\boldsymbol{\nabla}\mu_1$ which allows us to calculate $V^{\boldsymbol{\nu}} = \boldsymbol{\nu} \cdot \boldsymbol{\nabla}\mu_1$. Note, that knowledge of the normal velocity is sufficient to evolve the interface. For the numerical implementation we use a parametrization $\boldsymbol{z}_k(\alpha,\tau)$ for each Γ_k, where $\alpha \in [0, 2\pi]$. These parameter functions are evolved according to

$$\frac{d\boldsymbol{z}_k}{d\tau} = V_k^{\boldsymbol{\nu}}\boldsymbol{\nu}_k + V_k^{\mathbf{t}}\boldsymbol{t}_k\,. \tag{5.11}$$

where $\boldsymbol{\nu}_k$ and $\boldsymbol{t}_k$ denote the normal and tangent vectors w.r.t. the k-th precipitate. The tangential component $V_k^{\mathbf{t}}$ of $d\boldsymbol{z}_k/d\tau$ remains arbitrary and a special choice of the parametrization for the boundaries Γ_k will be used to simplify the numerical implementation. Here we follow [13] for the choice of the coordinate system, where θ_k is the angle of the tangent vector at points on Γ_k w.r.t. the x-axis and L_k denotes the length of the corresponding interface. The components of $\boldsymbol{z}_k(\alpha,\tau)$ are then replaced by the coordinates $s_{k\,\alpha}$ and θ_k through

$$s_{k\,\alpha} = |\boldsymbol{z}_k| \qquad \text{and} \qquad (\cos\theta_k(\alpha,\tau), \sin\theta_k(\alpha,\tau)) = \frac{(\mathrm{Re}\,(\boldsymbol{z}_k), \Im(\boldsymbol{z}_k))}{s_{k\,\alpha}} \tag{5.12}$$

so that the evolution equations

$$\frac{\partial s_{k\,\alpha}}{\partial\tau} = V_{k\,\alpha}^{\mathbf{t}} - \theta_{k\,\alpha}V_k^{\boldsymbol{\nu}} \qquad \text{and} \qquad \frac{\partial\theta_k}{\partial\tau} = \frac{V_{k\,\alpha}^{\boldsymbol{\nu}} + V_k^{\mathbf{t}}\theta_{k\,\alpha}}{s_{k\,\alpha}}\,. \tag{5.13}$$

are obtained. Note here, the index k refers to the k-th precipitate, while the index α denotes partial derivative w.r.t. the parameter α. Then the special choice of

$$V_k^{\mathbf{t}}(\alpha,\tau) = \int_0^\alpha \theta_{k\,\alpha'}\, V_k^{\boldsymbol{\nu}}\, d\alpha' - \frac{\alpha}{2\pi}\int_0^{2\pi} \theta_{k\,\alpha'}\, V_k^{\boldsymbol{\nu}}\, d\alpha' \tag{5.14}$$

yields the equal arclength parametrization

$$s_{k\,\alpha} = \frac{L_k(\tau)}{2\pi}\,, \qquad \text{for all } \alpha \tag{5.15}$$

and hence the simpler ODE-PDE system

$$\frac{\partial L_k}{\partial\tau} = -\int_0^{2\pi} \theta_{k\,\alpha'}\, V_k^{\boldsymbol{\nu}}\, d\alpha' \qquad \text{and} \qquad \frac{\partial\theta_k}{\partial\tau} = \frac{2\pi}{L_k}\left(V_{k\,\alpha}^{\boldsymbol{\nu}} + \theta_{k\,\alpha}\, V_k^{\mathbf{t}}\right)\,. \tag{5.16}$$

In summary, the complete boundary integral formulation for the evolution of the precipitates

is:

$$-\frac{1}{2}\Phi_k(\alpha,\tau)+\frac{1}{2\pi}\sum_{l=1}^{N}\int_0^{2\pi}\Phi_l(\alpha',\tau)\,\Im\left(\frac{\boldsymbol{z}_{l\,\alpha'}(\alpha')}{\boldsymbol{z}_l(\alpha')-\boldsymbol{z}_l(\alpha)}\right)d\alpha'+\frac{1}{L_k}\sum_{l=1}^{N}\int_0^{2\pi}\Phi_l(\alpha',\tau)\,d\alpha'$$

$$+\sum_{l=1}^{N}A_l\ln(\boldsymbol{z}_l(\alpha)-M_l)=\mu_1|_\Gamma\,, \tag{5.17}$$

$$\int_0^{2\pi}\Phi_k(\alpha',\tau)\,d\alpha'=0\qquad k=1,\ldots,N-1\,, \tag{5.18}$$

$$V_k^{\boldsymbol{\nu}}(\alpha,\tau)=-\frac{1}{L_k}\sum_{l=1}^{N}\int_0^{2\pi}\Phi_{l\,\alpha'}(\alpha',\tau)\,\mathrm{Re}\left(\frac{\boldsymbol{z}_{l\,\alpha}(\alpha)}{\boldsymbol{z}_l(\alpha')-\boldsymbol{z}_l(\alpha)}\right)d\alpha'\,, \tag{5.19}$$

together with (5.9), (5.14) and (5.16).

Now, onsider $\theta_{k\,\alpha}$ in in the second equation of (5.16). It gets another derivative in the first equation of (5.16) and another one in (5.17), since in θ, s_α coordinates the curvature in $\mu_1|_\Gamma$ is expressed as $\kappa=\theta_\alpha/s_\alpha$. Hence, there are three derivatives. Such high derivatives in an evolution equation will lead to numerically stiff problems (the stability constraint e.g. $\triangle t<O\left((\triangle x)^3\right)$ leads to prohibitive time stepping). However, the advantage of the above formulation is that the evolution equation can for each k be written as

$$\frac{\partial\theta}{\partial\tau}=\left(\frac{2\pi}{L}\right)^3\bar{\mu}\,\mathcal{H}\left[\theta_{\alpha\alpha\alpha}\right]+N(\alpha,\tau) \tag{5.20}$$

where

$$\bar{\mu}=\frac{1}{[u^{\pm}]}\int_0^{2\pi}\sigma\,d\theta\,. \tag{5.21}$$

The first term of (5.20) becomes in Fourier space

$$-\left(\frac{2\pi}{L}\right)^3|j|^3\,\theta \tag{5.22}$$

which is the stiffest term and will be treated implicitely. However, in this form it is linear and diagonal in Fourier space and hence one only has to solve a diagonal system. The remaining complicated nonlinear expression $N(\alpha,\tau)$ can be treated explicitely. We use a Pseudo-spectral method (using FFT) in space, and Leap-Frog for the explicit and Crank-Nicholson for the implicit time integration. The integration of the L_τ ODE is done with an Adams-Bashforth integrator. Equations (5.17), (5.18), (5.19) and (5.9) yield the Ψ and A_k. They represent a linear system and is solved iteratively using GMRES.

5.1 Examples

We are interested here in some first characteristic features of the influence of anisotropic surface tension on the dynamics of coarsening. This will be extended to include elastic effects in Part II.

For the numerical simulations we use for $A(\tilde{u})$ the linearly interpolating expression

$$A(\tilde{u}) = \begin{pmatrix} a^\alpha & 0 \\ 0 & a^\alpha \end{pmatrix} \tilde{u} + \begin{pmatrix} a_1^\beta & 0 \\ 0 & a_2^\beta \end{pmatrix} (1 - \tilde{u}) \,, \tag{5.23}$$

where the α-matrix corresponds to a cubic symmetry and the β-matrix to a tetragonal symmetry, frequently occuring in binary alloys, see e.g. [5]. For the configurational part of the free energy we choose a fourth order polynomial, i.e. $F'(\tilde{u}_\mathrm{o}) = \tilde{u}_\mathrm{o}(\tilde{u}_\mathrm{o} - 1/2)(\tilde{u}_\mathrm{o} - 1)$ so that $b_0 = 0$, $[u_\mathrm{o}^\pm] = 1$ and $G(v) = 1/4v^2(v-1)^2$. With this choice we obtain the following explicit expression for σ:

$$\sigma = \sqrt{a^\alpha} \frac{4}{105\, p^3} \left[(1-p)^{3/2}(4 - p - 3p^2) - 4 + 7p \right] \,, \tag{5.24}$$

$$\text{where} \quad p = q + \delta \sin^2\theta \quad \text{with} \quad q = \frac{a^\alpha - a_1^\beta}{a^\alpha}, \;\; \delta = \frac{a_2^\beta - a_1^\beta}{a^\alpha} \,. \tag{5.25}$$

For all simulations in the following three figures we let $q = 0.4$ and $\delta = 0.1$. For the initial conditions we always choose a pair of circles, one with center at the origin and of radius $R = 0.13$ and the other one with center shifted by $d > 2.01R$ from the origin and having 1% larger radius. We are interested in the effect of anisotropic surface tension and distance of the precipitates on the coarsening rate and their shape.

In the first figure 5 we see the change in area for two precipitates, intially of circular shape (solid line), where the center of the second one is shifted by $d = 5.2$ to the right and having 1% larger radius. In this figure we do not show the middle portion $0.2 < x < 5$ to better focus on the shape of the precipitates. For both precipitates, the growing (right) and the shrinking (left) one, coarsening proceeds by quickly assuming and retaining almost equilibrium shape (dotted lines), which can be found analytically as the stationary solution of (5.17)–(5.19), (5.9), (5.14) and (5.16), for a single precipitate

$$\begin{aligned} r_{1\,\mathrm{stat}} &= \int_0^s \cos\theta \, ds = \int_0^\theta \frac{\cos\theta}{\theta_s} \, d\theta = -\frac{1}{C}(\sigma \sin\theta + \sigma_\theta \cos\theta) \,, \\ r_{2\,\mathrm{stat}} &= \int_0^s \sin\theta \, ds = \int_0^\theta \frac{\sin\theta}{\theta_s} \, d\theta = \frac{1}{C}(\sigma \cos\theta - \sigma_\theta \sin\theta) \end{aligned} \tag{5.26}$$

with scaling factor C. In figure 6 the center of second precipitate is shifted only by $d = 0.325$ to the right. We see that the influence of diffusion dominates the shape of the precipitates. Only for very small precipiates is the equilibrium shape attained, i.e. when surface tension dominates, as seen for the smallest precipiate on the left. In the final figure we show the influence of distance of the precipitates on the coarsening rate, which is smaller for larger distances. Additionally, we performed a second set of simulations, where the center of the second precipitate had been placed a distance d above the origin instead to the right. While the influence of the distance on the shape is analogous to the previous examples, we also notice a dependence of the coarsening rate on the orientation of the precipitates with respect to each other. Figure 7 shows the area of the precipitates minus their initial area for three pairs initially with distance $d = 0.325$ (left), $d = 0.65$ (middle) and $d = 5.2$ (right). The solid lines represent pairs of precipitates, where the center of the second one is placed to the right of the origin, as in the previous figures, and

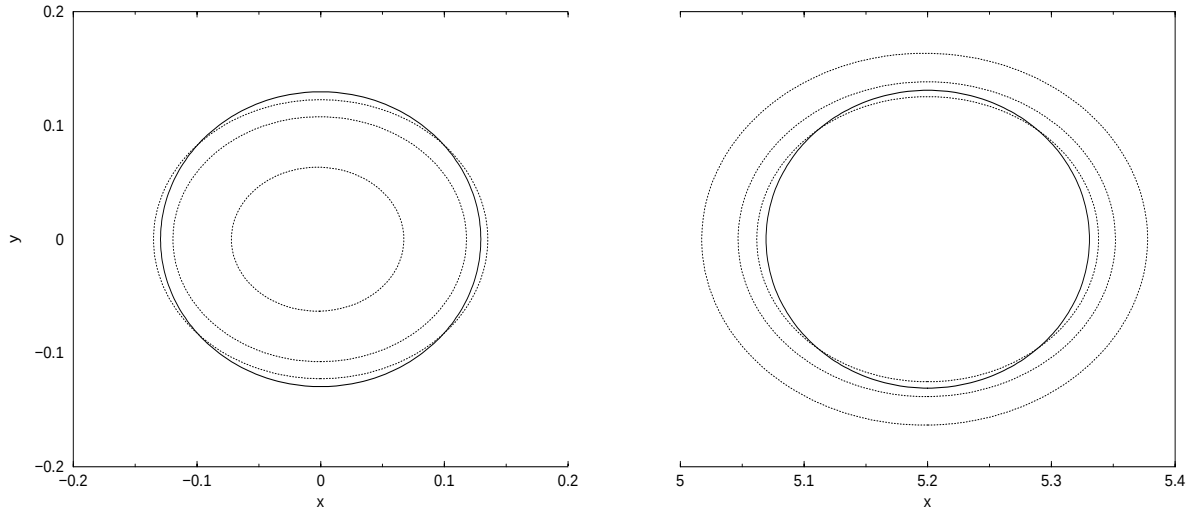

Figure 5: Two evolving precipitates with centers initially $d = 5.2$ apart (solid line). Middle portion $0.2 < x < 5.2$ not shown.

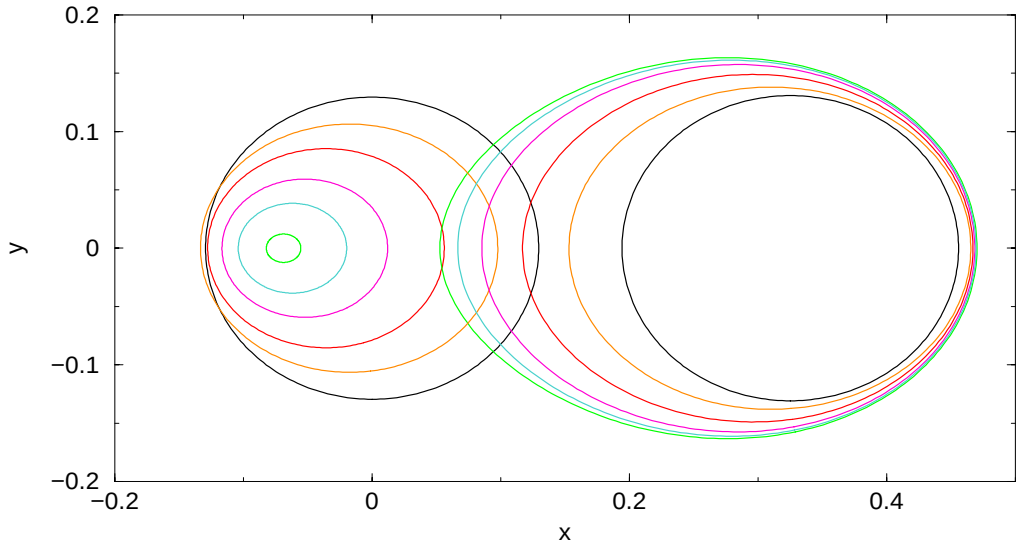

Figure 6: Two evolving precipitates with centers initially $d = 0.325$ apart.

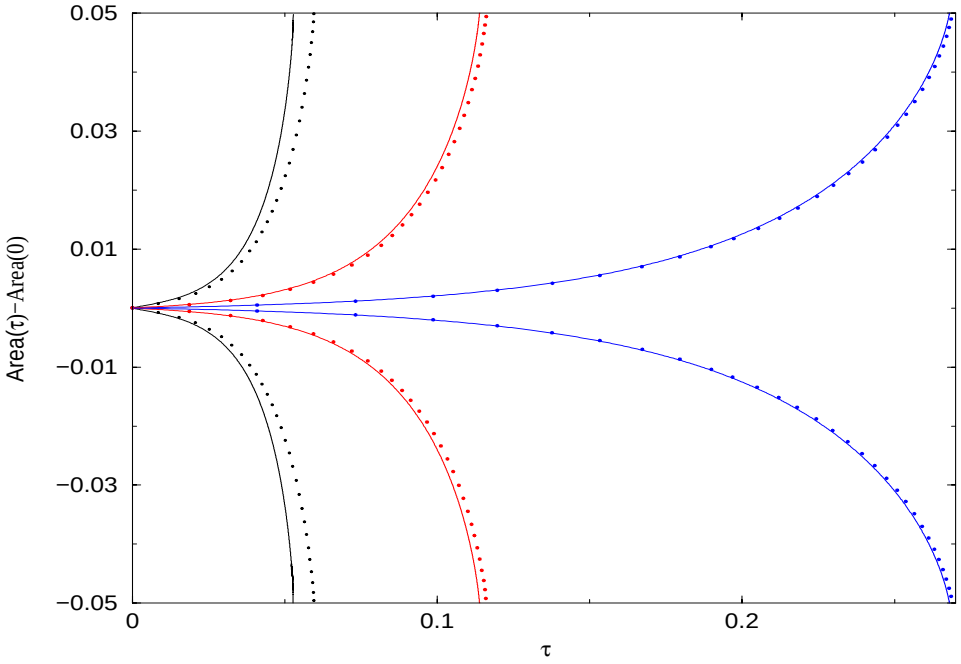

Figure 7: Change in area for two precipitates, placed next to each other (solid line) and over each other (dotted line).

the dotted lines represent those, where the center of the second precipitate is placed above the origin. We see that the effect of anisotropic surface tension on the coarsening is felt largely for nearby particles. Furthermore, we see a tendency that coarsening proceeds faster when the points of higher curvature are closer.

Acknowledgements

We would like to thank Harald Garcke for many stimulating discussions. BW would also like to thank Andreas Münch for very helpful comments on the numerical part of this study.

A Transformations

Suppose $\tilde{w}$ is a quantity defined in the inner coordinates (s, z, τ). Then its derivatives are related to the derivatives of the corresponding quantity w in outer coordinates via the invertible transformation matrix

$$M = \begin{pmatrix} & \mathrm{Q} & & 0 \\ & & & 0 \\ x_\tau & & y_\tau & 1 \end{pmatrix}, \quad \text{where} \quad Q = \begin{pmatrix} x_s & y_s \\ x_z & y_z \end{pmatrix} \tag{A.1}$$

by

$$\begin{pmatrix} \tilde{w}_s \\ \tilde{w}_z \\ \tilde{w}_\tau \end{pmatrix} = M \begin{pmatrix} w_x \\ w_y \\ w_\tau \end{pmatrix} \tag{A.2}$$

Since s is arclength

$$r_{1s}^2 + r_{2s}^2 = 1\,, \quad r_{1s} r_{1ss} + r_{2s} r_{2ss} = 0\,, \quad \kappa(s,\tau) = r_{1s} r_{2ss} - r_{2s} r_{1ss} \tag{A.3}$$

and

$$\mathbf{t}_s = \kappa \boldsymbol{\nu}\,, \quad \boldsymbol{\nu}_s = -\kappa \mathbf{t} \tag{A.4}$$

so that

$$r_{1ss} = -\kappa r_{2s}\,, \quad r_{2ss} = \kappa r_{1s} \tag{A.5}$$

Hence,

$$\boldsymbol{x}_s = (1 - \varepsilon\kappa)\mathbf{t}\,, \quad \boldsymbol{x}_z = \varepsilon \boldsymbol{\nu}\,, \quad \det Q = \varepsilon(1 - \varepsilon\, z\, \kappa)\,. \tag{A.6}$$

Now we can express the quantity w in the outer variables in terms of the inner variables by

$$\begin{pmatrix} w_x \\ w_y \\ w_\tau \end{pmatrix} = \begin{pmatrix} & \mathrm{Q}^{-1} & & 0 \\ & & & 0 \\ -\boldsymbol{x}_\tau \cdot \mathrm{Q}^{-1} & & & 1 \end{pmatrix} \begin{pmatrix} \tilde{w}_s \\ \tilde{w}_z \\ \tilde{w}_\tau \end{pmatrix} = \begin{pmatrix} r_{1s}(1+\varepsilon z\kappa) & -\varepsilon^{-1} r_{2s} & 0 \\ r_{2s}(1+\varepsilon z\kappa) & \varepsilon^{-1} r_{1s} & 0 \\ -V^{\mathbf{t}}(1+\varepsilon z\kappa) & -\varepsilon^{-1} V^{\boldsymbol{\nu}} & 1 \end{pmatrix} \begin{pmatrix} \tilde{w}_s \\ \tilde{w}_z \\ \tilde{w}_\tau \end{pmatrix}, \tag{A.7}$$

where we have used the approximation $1/(1 - \varepsilon z\kappa) = 1 + \varepsilon z\kappa + O(\varepsilon^2)$, and where we denote the tangential and normal velocity by

$$V^{\mathbf{t}} = \boldsymbol{x}_\tau \cdot \mathbf{t}\,, \quad V^{\boldsymbol{\nu}} = \boldsymbol{x}_\tau \cdot \boldsymbol{\nu}\,, \tag{A.8}$$

respectively.

The higher derivatives then transform as follows:

$$\begin{aligned} w_{xx} &= \varepsilon^{-2} r_{2s}^2 \tilde{w}_{zz} - \varepsilon^{-1}\left[\kappa r_{1s}^2 \tilde{w}_z + 2 r_{1s} r_{2s} \tilde{w}_{sz}\right] + r_{1s}^2 \tilde{w}_{ss} \\ &\quad -2\kappa r_{1s} r_{2s} \tilde{w}_s - z\kappa\left[\kappa r_{1s}^2 \tilde{w}_z + 2 r_{1s} r_{2s} \tilde{w}_{sz}\right] \qquad \text{(A.9)} \\ w_{yy} &= \varepsilon^{-2} r_{1s}^2 \tilde{w}_{zz} - \varepsilon^{-1}\left[\kappa r_{2s}^2 \tilde{w}_z - 2 r_{1s} r_{2s} \tilde{w}_{sz}\right] + r_{2s}^2 \tilde{w}_{ss} \\ &\quad +2\kappa r_{1s} r_{2s} \tilde{w}_s - z\kappa\left[\kappa r_{2s}^2 \tilde{w}_z - 2 r_{1s} r_{2s} \tilde{w}_{sz}\right] \qquad \text{(A.10)} \\ w_{xy} &= -\varepsilon^{-2} r_{1s} r_{2s} \tilde{w}_{zz} - \varepsilon^{-1}\left[\kappa r_{1s} r_{2s} \tilde{w}_z + \left(r_{2s}^2 - r_{1s}^2\right)\tilde{w}_{sz}\right] + r_{1s} r_{2s} \tilde{w}_{ss} \\ &\quad -\kappa\left(r_{2s}^2 - r_{1s}^2\right)\tilde{w}_s - z\kappa\left[\kappa r_{1s} r_{2s} \tilde{w}_z + \left(r_{2s}^2 - r_{1s}^2\right)\tilde{w}_{sz}\right] \qquad \text{(A.11)} \\ \triangle w &= \varepsilon^{-2}\tilde{w}_{zz} - \varepsilon^{-1}\kappa\tilde{w}_z + \tilde{w}_{ss} - z\kappa^2\tilde{w}_z \qquad \text{(A.12)} \end{aligned}$$

B Higher gradient coefficients

In this appendix we relate the coefficients, which appear in Eq. (2.13), to the three pair potentials φ_γ^{AA}, φ_γ^{BB}, φ_γ^{AB} and to the combinations (2.17), respectively. Recall the definitions $\Delta_i^{ab} = X_i^b - X_i^a$, $\Delta^{ab} = \mid X_i^b - X_i^a \mid$ and let us furthermore define $N_i = \Delta_i^{ab}/\Delta^{ab}$.

The coefficients determining the local part of the free energy read

$$\psi_\gamma^{AA} = \frac{1}{2}\sum_b \varphi_\gamma^{AA}(\Delta^{ab}), \quad \psi_\gamma^{\tilde{\varphi}} = \frac{1}{2}\sum_b \tilde{\varphi}_\gamma(\Delta^{ab}), \quad \psi_\gamma^{\varphi} = \frac{1}{2}\sum_b \varphi_\gamma(\Delta^{ab}). \tag{B.1}$$

The higher gradient coefficients, that we also call extended Cahn-Hilliard coefficients, read

$$a_{\gamma|kl}^{\varphi} = \frac{1}{2}\sum_b (\Delta^{ab})^2 \varphi_\gamma(\Delta^{ab}) N_k N_l, \quad a_{\gamma|kl}^{\tilde{\varphi}} = \frac{1}{2}\sum_b (\Delta^{ab})^2 \tilde{\varphi}_\gamma(\Delta^{ab}) N_k N_l, \tag{B.2}$$

and

$$A_{\gamma|klmnop}^{\varphi} = \frac{1}{2}\sum_b (\Delta^{ab})^4 \frac{\partial^2 \varphi_\gamma(\Delta^{ab})}{\partial \Delta_m^{ab} \partial \Delta_o^{ab}} N_k N_l N_n N_p, \quad A_{\gamma|klmnop}^{\tilde{\varphi}} = \frac{1}{2}\sum_b (\Delta^{ab})^4 \frac{\partial^2 \tilde{\varphi}_\gamma(\Delta^{ab})}{\partial \Delta_m^{ab} \partial \Delta_o^{ab}} N_k N_l N_n N_p. \tag{B.3}$$

Finally there are the coefficients which determine the elastic stiffness matrix, and these are

$$A_{\gamma|mnop}^{AA} = \sum_b (\Delta^{ab})^2 \frac{\partial^2 \varphi_\gamma^{AA}(\Delta^{ab})}{\partial \Delta_m^{ab} \partial \Delta_o^{ab}} N_k N_l, \quad A_{\gamma|mnop}^{\varphi} = \sum_b (\Delta^{ab})^2 \frac{\partial^2 \varphi_\gamma(\Delta^{ab})}{\partial \Delta_m^{ab} \partial \Delta_o^{ab}} N_k N_l,$$

$$A_{\gamma|mnop}^{\tilde{\varphi}} = \sum_b (\Delta^{ab})^2 \frac{\partial^2 \tilde{\varphi}_\gamma(\Delta^{ab})}{\partial \Delta_m^{ab} \partial \Delta_o^{ab}} N_k N_l. \tag{B.4}$$

We conclude that all the constitutive law of the phase field model from the above can be determined from three pair potential function. How these functions can be fitted to experimental data is described in [6].

References

[1] J. W. Cahn, J. E. Hilliard, Free energy of a nonuniform system. I. Interfacial free energy, *J. Chem. Phys.*, Vol. 28(1), pp. 258–267, 1958

[2] D. W. Hoffmann, J. W. Cahn, J. E. Hilliard, A vector thermodynamics for anisotropic surfaces I: Fundamentals and applications to plane surface junctions, *Surace Sciences*, Vol. 31, 1972

[3] J. W. Cahn, D. W. Hoffmann, A vector thermodynamics for anisotropic surfaces II: Curved and faceted surfaces, *Acta Met.*, Vol. 22, 1974

[4] J. W. Cahn, A. Novick-Cohen, Evolution equations for phase separation and ordering in binary alloys, *J. Stat. Phys.*, Vol. 76, pp. 877–909, 1994

[5] W. Dreyer, W. H. Müller, A study of the coarsening in tin/lead solders, *Int. J. Solid Struct.*, Vol. 37(28), pp. 3841–3871, 2000

[6] W. Dreyer, W. H. Müller, Modeling diffusional coarsening in eutectic tin/lead solders: A quantitative approach, *Int. Journal of Solids and Structures*, 2000

[7] W. Dreyer, W. H. Müller, EAM potential, *WIAS preprint*, 2003

[8] W. Dreyer, M. Kunik, Cold, thermal and oscillator closure of the atomic chain, *J. Phys. A: Math. Gen.*, Vol. 33(10):2097–2129 (2000)

[9] W. Dreyer, On jump conditions at phase boundaries, *WIAS preprint* No. 869, 2003

[10] D. de Fontaine, Clustering effect in solid solutions, in: *Treatise on Solid State Chemistry*,N.B. Hannah (Editor), PLenum Press New York, London, pp. 129-178 (1975)

[11] H. Garcke, B. Nestler, B. Stoth, On anisotropic order parameter models for multiphase systems and their sharp interface limits, *Physica D*, Vol. 115, pp87–108, 1998.

[12] H. J. Jou, P. H. Leo, J. S. Lowengrub, Microstructural Evolution in Inhomogeneous Elastic Media, *J. Comp. Phys.*, Vol. 131, pp. 109–148, 1997

[13] H. J. Hou, J. S. Lowengrub, M. J. Shelley, Removing the stiffness from interfacial flows with surface tension, *J. Comp. Phys.*, Vol. 114, pp. 312–338, 1994

[14] G. Leibfried, Gittertheorie der mechanischen und thermischen Eigenschaften der Kristalle, *Encyclopedia of Physics*, Vol. VII, Part I, Crystal Physics I, Springer Verlag, 1955

[15] P. H. Leo, J. S. Lowengrub, Qing Nie, Microstructural evolution in orthotropic elastic media, *J. Comp. Phys.*, Vol. 157, pp. 44–88, 2000

[16] S. G. Mikhlin, Integral equations and their applications to certain problems in Mechanics, Mathematical Physics, and Technology, *Pergamon New York*, 1957

[17] I. Müller, Thermodynamics *Interaction of mechanics and Mathematics*, Pitman Advanced Publishing Program, 1985

[18] R. L. Pego, Front migration in the nonlinear Cahn-Hilliard equation, *Proc. R. Soc. Lond. A*, Vol. 422, pp. 261–278, 1989.

[19] I. Steinbach, F. Pezolla, B. Nestler, M. Seeßelberg, R. Prieler, G. J. Schmitz, J. L. L. Rezende, A phase-field concept for multiphase systems, *Physica D*, 1996, pp. 135–147.

[20] A. A. Wheeler, G. B. McFadden, W. J. Boettinger, Phase-field model for solidification of a eutectic alloy, *Proc. R. Soc. Lond. A*, Vol. 452, pp. 495–525, 1996.